
ETD Archive

2019

Thenar Muscle and Transverse Carpal Ligament Relationship

Jeremy Granieri Loss
Cleveland State University

Follow this and additional works at: <https://engagedscholarship.csuohio.edu/etdarchive>

 Part of the [Biomechanics and Biotransport Commons](#)

How does access to this work benefit you? Let us know!

Recommended Citation

Loss, Jeremy Granieri, "Thenar Muscle and Transverse Carpal Ligament Relationship" (2019). *ETD Archive*. 1164.

<https://engagedscholarship.csuohio.edu/etdarchive/1164>

This Thesis is brought to you for free and open access by EngagedScholarship@CSU. It has been accepted for inclusion in ETD Archive by an authorized administrator of EngagedScholarship@CSU. For more information, please contact library.es@csuohio.edu.

THENAR MUSCLE AND TRANSVERSE CARPAL LIGAMENT RELATIONSHIP

JEREMY LOSS

Bachelor of Science in Mechanical Engineering

University of Notre Dame

May 2017

Submitted in partial fulfillment of requirements for the degree

MASTERS OF SCIENCE IN BIOMEDICAL ENGINEERING

at

CLEVELAND STATE UNIVERSITY

May 2019

We hereby approve this thesis

For

JEREMY LOSS

Candidate for the Master of Science in Biomedical Engineering degree

for the Department of

Chemical and Biomedical Engineering

And

CLEVELAND STATE UNIVERSITY'S

College of Graduate Studies by

Thesis Chairperson, Dr. Zong-Ming Li
Department of Biomedical Engineering, Cleveland Clinic

Date

Thesis Committee Member, Dr. Christopher L. Wirth
Department of Chemical and Biomedical Engineering, Cleveland State University

Date

Thesis Committee Member, Dr. Eric M. Schearer
Department of Mechanical Engineering, Cleveland State University

Date

Date of Defense: April 30, 2019

ACKNOWLEDGEMENTS

There are so many individuals who have provided their intellectual, spiritual, social, and emotional support throughout this process. I would like to first thank Dr. Zong-Ming Li for providing me the opportunity, time, and resources to pursue this degree. I want to thank all of the members of the Hand Research Lab at the Cleveland Clinic, specifically Rakshit Shah, Hui Zhang, and Kishor Lakshminarayanan, as well as Matthew Rudy and previous members Carli Norman, Emily Grandy, Lenicia Jenkins, Yifei Yao, Narenraj Selvaraj, and Brinda Pogul for their intellectual input and companionship during my time in the lab. I want to especially thank my parents (John and Melanie), my brothers (Ronald, Michael, Dominic, and Patrick), and my fiancé (Sarah Ramsperger) for their constant love, support, and encouragement. I am grateful to Dr. Peter J. Evans, Andrew Steckler, and Dr. Richard L. Drake for offering their time and expertise in the pursuit of my degree. Finally, I would like to thank the members of my thesis committee (Dr. Zong-Ming Li, Dr. Christopher L. Wirth, Dr. Eric M. Schearer) for taking the time to guide me during my thesis research.

THENAR MUSCLE AND TRANSVERSE CARPAL LIGAMENT RELATIONSHIP

JEREMY LOSS

ABSTRACT

The transverse carpal ligament (TCL) acts as a partial origin for the thenar muscles (abductor pollicis brevis (APB), flexor pollicis brevis (FPB), opponens pollicis (OPP)). The attachment between the thenar muscles and TCL implies a relationship between the tissues. The thenar muscles rely on their origins for thumb motion and force production. However, individual thenar origin information is lacking. Further information regarding the anatomical relationship between the individual thenar muscles and TCL may provide insight into thenar muscle function. In addition, the TCL responds to thenar muscle contraction as shown by volar migration of the TCL during various thumb movements. However, the muscle-ligament biomechanical interaction after TCL transection is unknown. Further understanding of the altered muscle-ligament biomechanical relationship may illuminate the consequence of surgical procedures on this interaction.

The overall goal of this thesis was to investigate the relationship between the thenar muscles and the transverse carpal ligament. First, the individual thenar muscle origins were identified through cadaveric dissection and digitized to determine the individual thenar muscle's anatomical relationship to the TCL. Second, cadaveric muscle loading was used to mimic thenar muscle contractions in intact and released specimens to examine the consequences of TCL release on the muscle-ligament biomechanical relationship. The results showed that each muscle had distinct origin size and location, with the OPP having the largest origin size and the APB with the most proximal location. The APB originated mainly on the TCL while the OPP and FPB originated mostly off the TCL. It was also observed that muscle loading after TCL release caused different patterns of muscle-ligament interaction compared to loading before release. However, the noted difference in muscle-ligament interaction was inconclusive.

The current investigations advance our understanding of the anatomical configuration at the interface between the TCL and individual thenar muscles and imply a possible consequence of TCL transection with regards to muscle-ligament biomechanical interaction. Our findings may be applied to explain other clinical implications of muscle-ligament interaction and may influence future studies focused on illuminating the pathomechanical effect of TCL transection.

TABLE OF CONTENTS

	Page
ABSTRACT.....	iv
LIST OF TABLES	viii
LIST OF FIGURES	ix
CHAPTER	
I. BACKGROUND.....	1
1.1 Anatomy of the Thenar Muscles	1
1.2 Anatomy of the Transverse Carpal Ligament and Carpal Tunnel....	2
1.3 Biomechanical Role of the TCL.....	2
1.4 Development of Carpal Tunnel Syndrome.....	3
1.5 Interventions for CTS Symptom Relief.....	3
1.6 Complications of CTR.....	4
1.7 Why Study Alteration of Muscle-Ligament Interaction after CTR?	4
II. SPECIFIC AIMS.....	6
III. INDIVIDUAL THENAR MUSCLE ORIGINS ON THE TRANSVERSE	
CARPAL LIGAMENT.....	8
3.1 Introduction	8
3.2 Methods	10
3.3 Results	16
3.4 Discussion	21
IV. BIOMECHANICAL INTERACTION BETWEEN THE MUSCLE AND	
LIGAMENT AFTER TRANSVERSE CARPAL LIGAMENT RELEASE	25

4.1 Introduction	25
4.2 Methods	27
4.3 Results	33
4.4 Discussion	36
V. CONCLUSIONS.....	41
REFERENCES	43

LIST OF TABLES

Table	Page
I. Selected loading magnitudes for individual thenar muscles	31

LIST OF FIGURES

Figure	Page
1. Overall thesis approach.....	7
2. Specimen dissection showing (a) partial and (b) complete removal of the OPP	11
3. Complete specimen dissection and tracing. H: hamate, T: trapezium, S: scaphoid, P: pisiform.	11
4. Experimental apparatus for specimen digitization.....	12
5. Specimen digitization.....	13
6. Transformation of digitized data from the Microscribe coordinate system to the anatomical coordinate system	14
7. TCL mesh generation from (a) dataset to (b) mesh	15
8. A representative reconstruction of the combined TCL and muscle origin meshes. Bright shades of each color represent origin on the TCL. Dull shades of each color represent origin off the TCL.	15
9. Individual muscle origin areas	17
10. Origin area on and off the TCL normalized by muscle origin area	18
11. TCL space occupied by each muscle	19
12. Muscle origin centroid location in the radial-ulnar and proximal-distal directions. H: hamate, T: trapezium, S: scaphoid, P: pisiform	20
13. Incision path for dissection. Dotted yellow lines were used to direct the path of incision (white).	28
14. Post osteotomy clamping of the first metacarpal used for OPP loading.....	28
15. Experimental set-up for thenar muscle loading	29
16. Specimen secured in experimental apparatus	30
17. Quantification of carpal arch height, width, and area from traced hamate, trapezium, and volar TCL border.....	33

18. Normalized CAH for the intact and released trials. A: APB, F: FPB, O: OPP, A+F: APB-FPB, A+O: APB-OPP, F+O: FPB-OPP, L: ALL 35
19. Normalized CAW for the intact and released trials. A: APB, F: FPB, O: OPP, A+F: APB-FPB, A+O: APB-OPP, F+O: FPB-OPP, L: ALL 35
20. Normalized CAA for the intact and released trials. A: APB, F: FPB, O: OPP, A+F: APB-FPB, A+O: APB-OPP, F+O: FPB-OPP, L: ALL 36

CHAPTER I

BACKGROUND

1.1 Anatomy of the Thenar Muscles

The muscles on the palmar side of the hand responsible for generating thumb motion and forces¹ are referred to as the thenar muscles. The three muscles associated with this group are the abductor pollicis brevis (APB), flexor pollicis brevis (FPB), and opponens pollicis (OPP). The APB is the most volar of the three muscles, originating from the TCL as well as the tubercle of the trapezium and the scaphoid, and inserting into the volar base of the thumb proximal phalanx.² The APB plays a large role in abduction of the thumb and assists the FPB in thumb proximal phalanx flexion.³ The FPB lies distal to the APB and consists of two muscle heads. Both FPB heads insert at the base of the thumb proximal phalanx, but the deep head originates from the dorsal aspect of the distal carpal bones, while the superficial head anchors into the TCL and distal edge of ridge of trapezium.^{2,4} Flexion of the carpometacarpal (CMC) and metacarpophalangeal (MCP) joints, as well as initiating thumb rotation for opposition, are the primary biomechanical functions of the FPB.^{2,3} The OPP is the most dorsal of the three muscles, inserting along the volar aspect of the first metacarpal and originating from the transverse carpal ligament (TCL) and ridge of trapezium.^{2,4} The OPP plays a major role in generating

opposition of the thumb.³ Altogether, 68% of total thenar muscle origins have been reported to lie on the TCL.⁵

1.2 Anatomy of the Transverse Carpal Ligament and Carpal Tunnel

The transverse carpal ligament (TCL) is a collagenous tissue in the wrist bordered proximally by the flexor retinaculum and distally by the palmar aponeurosis.⁶ The boundaries of the TCL have been identified by its bony attachment sites on the hook of hamate, tubercle of the trapezium, pisiform, and scaphoid.⁷⁻⁹ The TCL forms the volar border of the carpal tunnel: a fibro-osseous passageway containing nine flexor tendons and the median nerve. The curve formed by the TCL is referred to as the carpal arch. The area between the TCL curve and the TCL's bony attachments is referred to as carpal arch area. The length of the straight line between the TCL's attachments on the hook of hamate and the ridge of trapezium is defined as carpal arch width, and the perpendicular distance from the most volar aspect of the TCL to this line is the carpal arch height.

1.3 Biomechanical Role of the TCL

As a boundary for the carpal tunnel, the TCL plays a large role in the carpal tunnel's biomechanical functions. Specifically, the TCL provides compliance¹⁰ and structural stability¹¹ to the carpal tunnel. The structural enclosure by the TCL constrains the volar migration of the carpal tunnel contents.¹² TCL-generated constraint contributes to the pulley motion of the flexor tendons¹³ and prevents bowstringing of the flexor tendons that pass through the carpal tunnel¹⁴. In addition to the TCL's biomechanical roles as part of the carpal tunnel, the TCL anchors the APB, OPP, and the superficial head of the FPB.⁵ The thenar muscle anchoring on the TCL allows for thenar force production during thumb activities, such as pinching¹⁵ and pipetting¹⁶.

1.4 Development of Carpal Tunnel Syndrome

Compression of the median nerve within the carpal tunnel can lead to the onset of Carpal Tunnel Syndrome, or CTS. CTS is the most common nerve compression neuropathy, affecting between 3-5% of the general population.^{17,18} Patients afflicted by CTS report numbness, pain, tingling, and loss of sensation in their median nerve innervated digits¹⁹. Multiple etiologies of CTS have been proposed, such as alterations of the TCL's material properties²⁰⁻²² or hypertrophy of the flexor tendon synovium²³.

1.5 Interventions for CTS Symptom Relief

Conservative treatments for CTS range from splinting and physical therapy to steroid injections and NSAIDs. Though these interventions are commonly prescribed for treating mild or moderate cases of CTS, the long-term clinical efficacy of conservative treatments is minimal.²⁴ When conservation approaches cannot provide long-term CTS symptom relief or symptoms become more severe, patients elect to undergo carpal tunnel release (CTR) surgery. During CTR, the TCL is either partially or fully transected in an effort to increase carpal tunnel volume and reduce intratunnel pressure. An array of different CTR techniques have been developed, such as open release, minimally invasive release²⁵, endoscopic release²⁶, TCL flap reconstruction²⁷, and “z-plasty” reconstruction²⁸. In the US alone, 450,000 carpal tunnel releases are performed annually with an associated cost of \$2 billion US dollars.²⁹ Surgical interventions have been shown to provide symptom relief for patients with moderate to severe symptoms³⁰ and are more effective in providing long-term symptom relief than conservative treatments³¹.

1.6 Complications of CTR

Though patients who undergo CTR report symptom relief post-surgery, complications still arise. Incomplete release of the TCL is a common complication of endoscopic carpal tunnel release³², reducing the effectiveness of endoscopic CTR^{33,34} and leading to future surgical revisions³⁵. As well, anatomical variations in the course of both the motor branch of the median nerve and muscle origins on the TCL interfere with surgical intervention, and significant alterations in hand function can occur if these variations are not accounted for.³⁶⁻⁴⁰ Scar tissue pain and median nerve fibrosis⁴¹ as well as return of pre-surgery symptoms⁴² are other common complications after CTR.

Moreover, TCL transection significantly affects the TCL's biomechanical functions. Transection of the TCL reduces the stability of the carpal bones^{43,44} and alters the contact forces of the carpal bones⁴⁵. The removal of the TCL's volar constraint on the tunnel's content diminishes the pulley motion of the flexor tendons and allows for greater flexor tendon volar excursion, reducing pinch and grip strength after surgery^{46,47} and increasing the frequency of trigger finger in CTR patients⁴⁸. Long-term thenar muscle function is also affected by TCL transection, as the effective contraction length of the muscle is decreased after surgery⁴⁹ leading to reduction in overall muscle length and strength. Though the effect of TCL transection on thenar muscle function is known, little research has focused on how TCL transection alters the biomechanical interaction between the thenar muscles and the TCL.

1.7 Why Study Alteration of Muscle-Ligament Interaction after CTR?

As discussed, the APB, OPP, and superficial head of the FPB originate from the volar surface of the TCL^{2,5} and utilize this anchoring to generate thumb movements¹.

Therefore, thenar muscle function is reliant on biomechanical interaction between the thenar muscles and the TCL, and this muscle-ligament interaction is derived from the thenar muscle origins on the TCL. Transection of the TCL during CTR could not only disrupt the ligament structure per se, but may also alter thenar muscle anchoring, interfere with the function of the thenar muscles, and generate new patterns of muscle-ligament interaction. New patterns of muscle-ligament interaction could provide evidence of post-release complications such as the reduction in CTR patient grip strength.⁴³ Therefore, understanding of muscle-ligament interaction after TCL release can provide the biomechanical information to fully encapsulate the biomechanical consequences of CTR.

CHAPTER II

SPECIFIC AIMS

The transverse carpal ligament (TCL) acts as a partial origin for the thenar muscles, and this attachment generates a relationship between the thenar muscles and the TCL. The thenar muscles derive their function from their origins. However, information regarding the individual thenar muscle origins is lacking. Greater understanding of the anatomical relationship between the individual thenar muscles and the TCL can provide insight into the function of the individual thenar muscles. Additionally, the TCL responds to thenar muscle contraction by migrating volarly as shown during pinching¹⁵ and pipetting¹⁶ tasks. These studies investigated the biomechanical interactions between the thenar muscles and TCL in intact TCLs, but not in released TCLs. Transection of the TCL is a common surgical procedure for relieving CTS symptoms. Further muscle-ligament biomechanical information after TCL transection may illuminate another biomechanical consequence of surgical intervention. Therefore, the overall goal of this thesis is to investigate the relationship between the thenar muscles and the transverse carpal ligament (Figure. 1). This goal will be achieved through the following two aims:

Aim 1: To investigate the size and location of the individual thenar muscle origins both on and off the TCL. We hypothesized that each muscle will have distinct origin size and location. Origin size and location will be quantified by its area and centroid, respectively.

Aim 2: To examine the effect of TCL release on muscle-ligament interaction. We quantified the effect of TCL release by measuring the morphological parameters of the TCL-formed carpal arch before and after thenar muscle loading in intact and released specimens. We hypothesized that changes in arch height, width, and area will be significantly affected by TCL release.

This thesis will provide critical insight regarding the anatomical and biomechanical relationships between the thenar muscles and the TCL. The first aim of this thesis will expand the anatomical understanding of the individual thenar muscle origins for future study of muscle-ligament interaction implications. The second aim of this thesis will elucidate a possible pathomechanical consequence of TCL transection.

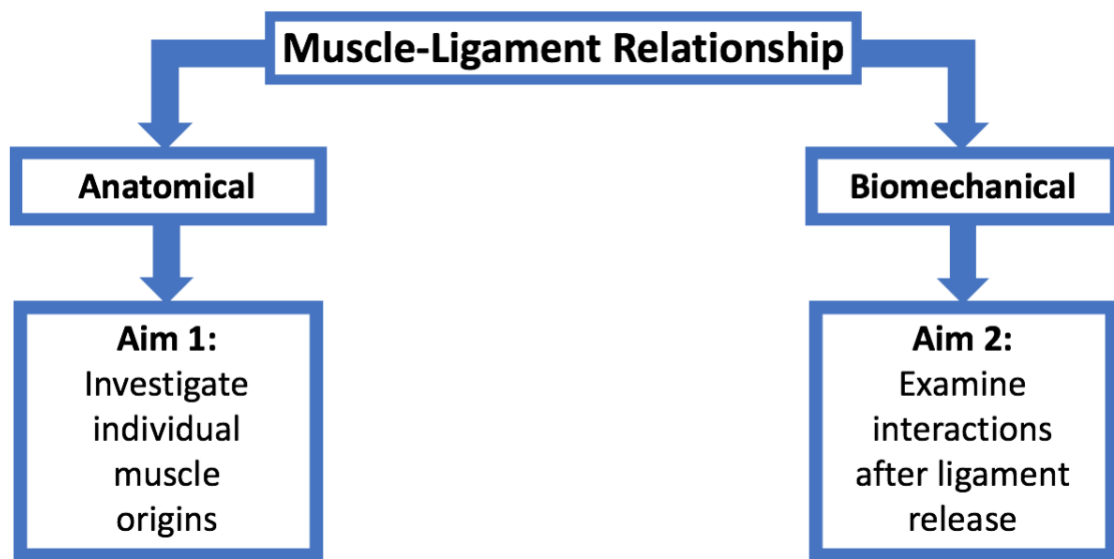


Figure 1. Overall thesis approach

CHAPTER III

INDIVIDUAL THENAR MUSCLE ORIGINS ON THE TRANSVERSE CARPAL LIGAMENT

3.1 Introduction

The transverse carpal ligament (TCL), in addition to its role as a carpal tunnel boundary, acts as an anchor for the three thenar muscles: the abductor pollicis brevis (APB), flexor pollicis brevis (FPB), and opponens pollicis (OPP).^{2,4} The APB rests on top of both the FPB and OPP, while the FPB lies distal and slightly ulnar to the APB and the OPP lies the most dorsal of the three muscles.³ The anatomical arrangement of the muscle origins dictates the biomechanical functions of the muscles^{1,50} as well as the biomechanical interaction between the thenar muscles and the TCL^{15,16}.

Previous research regarding the thenar muscle origins discusses their size and location broadly.² Few studies have quantified the size and location of the thenar muscle origins.^{5,51} Kung et al.⁵ quantified the overall origin size of the thenar and hypothenar muscles in cadaveric specimen and determined that 68% of the thenar muscles originate from the TCL. However, minimal information regarding the individual muscle origins is available.⁵¹ Moreover, the percentage of thenar muscle originating from the TCL has been reported⁵, but the percentage of total TCL area occupied by each thenar muscle has

yet to be investigated. Finally, no previous research has reported the centroids of the individual thenar muscle origins. Therefore, further studies on the size and location of the individual thenar muscle origins are necessary.

Additional information regarding individual thenar muscle origin size and location can be applied to better understand the biomechanical implications of thenar muscle interaction with the TCL. For example, repetitive muscle-ligament interaction could alter the material properties of the TCL⁵²⁻⁵⁴, leading to increases in TCL thickness and stiffness. Changes to the TCL's material properties has been suggested as a possible etiology for CTS.²⁰⁻²² Understanding the size and location of the individual muscle origins could indicate how each muscle's activation may play a role in the development of CTS. In addition, thenar muscle contraction volarly migrates the TCL^{15,16} and has been suggested for use in carpal arch space augmentation for relieving median nerve compression. Individual thenar muscle origin size and location information could indicate which muscles have the greatest potential interaction with the TCL and may direct future intervention strategies. Finally, CTS patients elect to undergo carpal tunnel release (CTR) surgery, during which the TCL may be fully or partially transected to increase carpal tunnel volume. Alteration to the TCL affects the anchoring of the thenar muscles, which may explain post-operative complications such as weakened grip strength.⁴³ An in-depth understanding of the individual thenar muscle origins could provide insight into this possible biomechanical mechanism underlying the undesirable consequence of surgical procedures.

Therefore, the aim of this study was to further investigate the size and location of the individual thenar muscle origins both on and off the TCL. Muscle origin information

was collected through digitization of cadaveric specimens and examined using three-dimensional mesh generation. We hypothesized that each muscle will have distinct origin size and location. Origin size and location will be quantified by its area and centroid, respectively.

3.2 Methods

Specimens: Ten freshly-frozen female cadaveric specimens (all left hands, mean age 74.2 ± 13.0 years; mean BMI 22.2 ± 4.1 kg/m²) were examined in this study.

Dissection Preparation: Prior to dissection, each specimen was removed from a storage freezer and thawed for at least 12 hours to room temperature. All specimens were volarly dissected to expose the TCL, bony attachment sites of the TCL (hook of hamate, ridge of trapezium, tubercle of the scaphoid, and pisiform), and thenar muscle origins. The skin, fat, and fascia above the TCL were removed, and any non-thenar tissues were cleaned off the TCL's surface. Care was taken to maintain the integrity of the thenar muscle origins on the TCL's surface. The flexor tendons and median nerve were dissected distal to the carpal tunnel and removed proximally from the tunnel. Each muscle's insertion was dissected to allow reflection of the muscle body for complete visualization of the muscle's origins. The boundary of each muscle origin was traced using a marker (Figure. 2a), and the muscle was completely dissected (Figure 2b). The TCL surface was identified as the tissue within the four bony TCL attachment sites.⁷⁻⁹ TCL boundaries were traced using lines passing through the bony attachment sites (Figure. 3). The TCL bony attachment sites were also marked on each specimen.

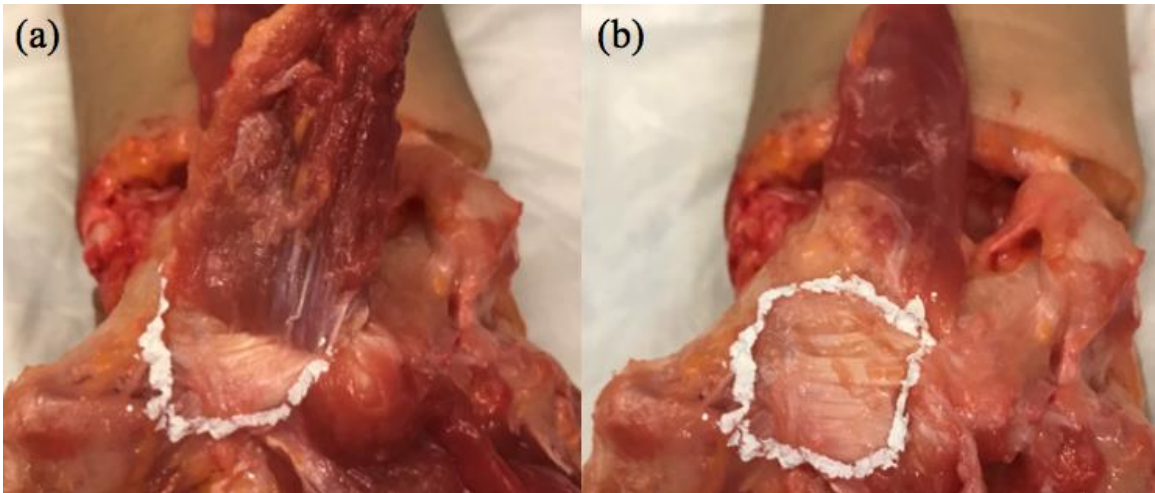
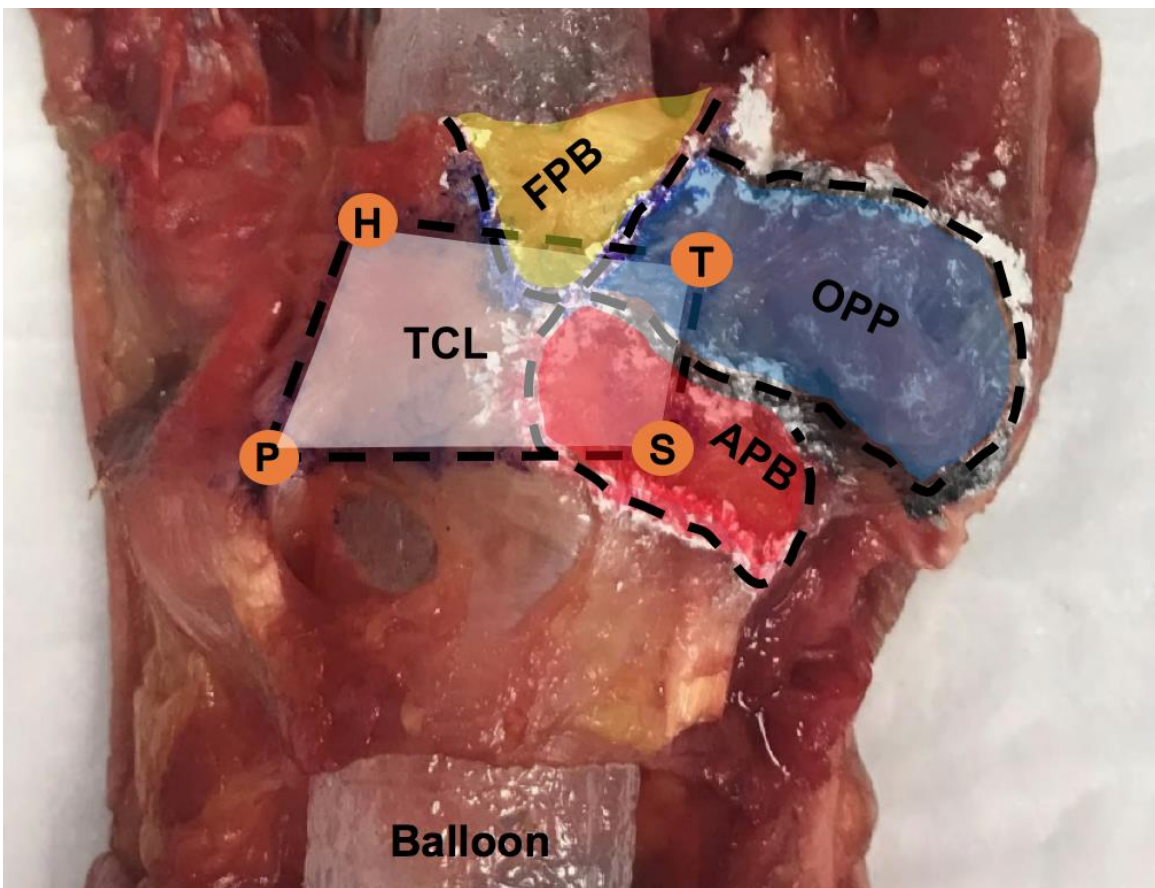


Figure 2. Specimen dissection showing (a) partial and (b) complete removal of the OPP



● TCL-bone attachment sites

Figure 3. Complete specimen dissection and tracing. H: hamate, T: trapezium, S: scaphoid, P: pisiform.

Apparatus: An inflatable balloon (Vention Medical Inc., Denver, CO, USA) was placed within the carpal tunnel, and a simulated physiological pressure of 24 mmHg⁵⁵ using air was maintained throughout testing. Each specimen was secured in a custom-made thermoplastic splint with the wrist in an anatomically neutral position. The digits were stabilized using Velcro straps with the fingers extended and the thumb in abduction. A custom-made apparatus was used to secure the specimen and digitizer throughout data collection (Figure. 4). A three-dimensional digitizer (Microscribe GX2, Immersion Corp., San Jose, CA, USA) was attached to a wooden board through a screw in the digitizer's base. A Velcro strip on the opposite end of the board secured the splint during testing.

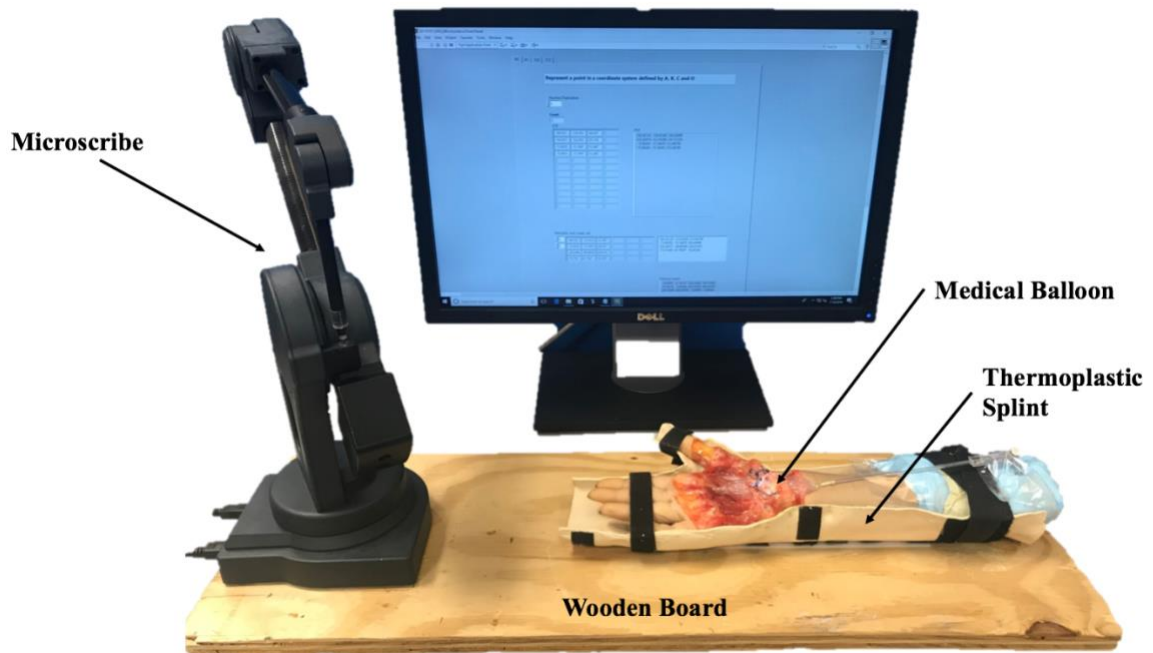


Figure 4. Experimental apparatus for specimen digitization

Digitization: Three trials of the TCL volar surface and each muscle origin were collected. The border of each tissue was first collected to define the boundary of the dataset. Multiple digitization passes of the TCL volar surface and muscle origins were

performed within each trial to generate a dense cloud of surface points. Care was taken to ensure light touch of the digitizer tip on all tissues so the contour of the tissue surfaces would not be disrupted (Figure. 5). Finally, the four TCL bony attachment sites were digitized for use in generating a local coordinate system.

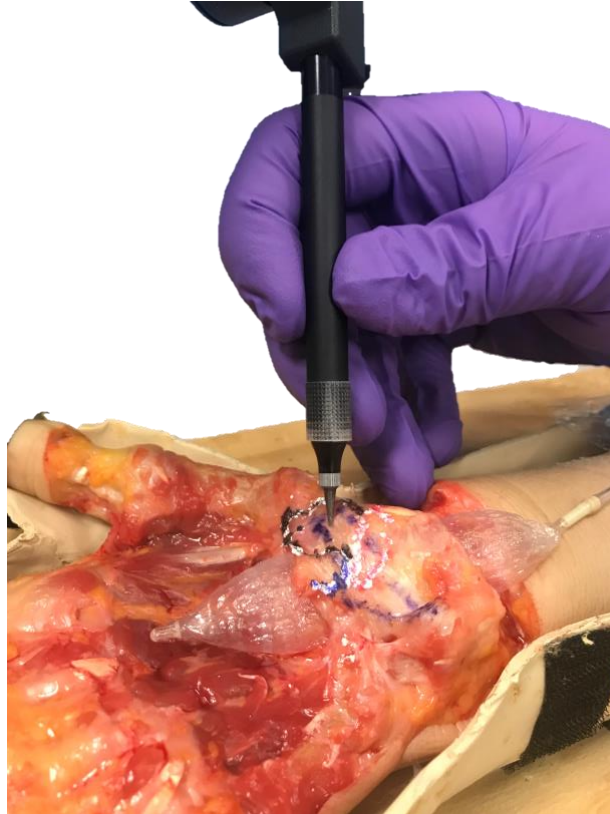


Figure 5. Specimen digitization

Data Processing: To gain an anatomical perspective of the muscle origins, a local anatomical coordinate system was established using the digitized locations of the trapezium, hamate, and scaphoid. The origin of the coordinate system was placed on the ridge of trapezium and its x-axis, y-axis, and z-axis laid in the radio-ulnar, proximal-distal, and volar-dorsal directions of the wrist, respectively. Using a previously established method⁵⁶, a transformation matrix was calculated to convert the collected data

from the Microscribe coordinate system to the local anatomical coordinate system. All digitized data was converted to the anatomical coordinate system using a custom LabVIEW (National Instruments, Austin, TX, USA) program (Figure. 6).

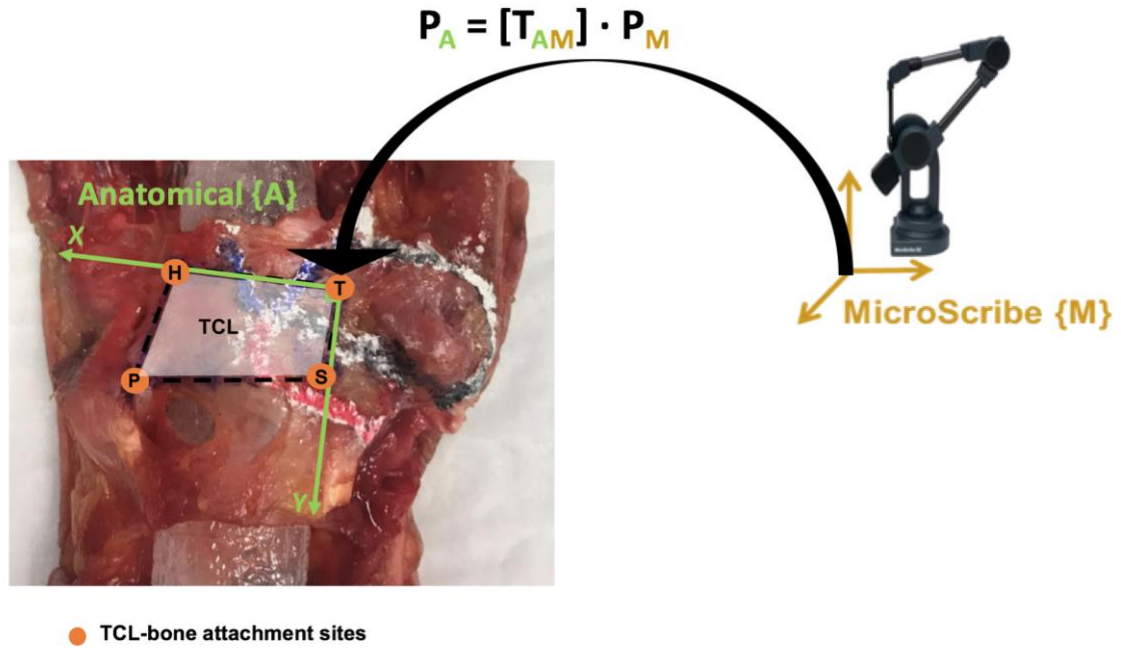


Figure 6. Transformation of digitized data from the Microscribe coordinate system to the anatomical coordinate system

Rhinoceros 3D (Robert McNeel & Associates, Seattle, WA, USA) was then utilized to generate meshes for the TCL and muscle origins. The most populated trial for each tissue was selected for mesh generation (Figure. 7a). The outermost data points representing the border of the tissue were first connected using the “polyline” function to generate the boundary of the dataset. The “Patch” command was then used to generate a surface passing through the dataset, and the generated surface was trimmed using the boundary of the dataset. A mesh from the remaining surface was then created (Figure.

7b). Once meshes for the TCL and the three muscles were generated, the four meshes were combined into a single file for data analysis (Figure. 8).

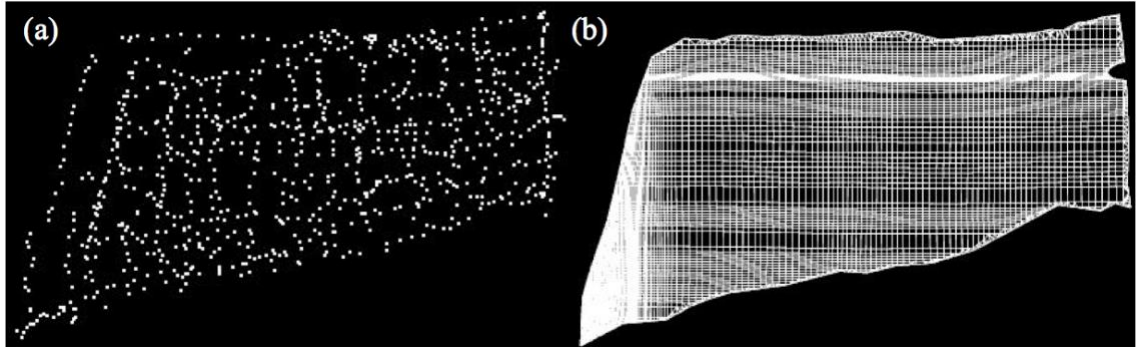


Figure 7. TCL mesh generation from (a) dataset to (b) mesh

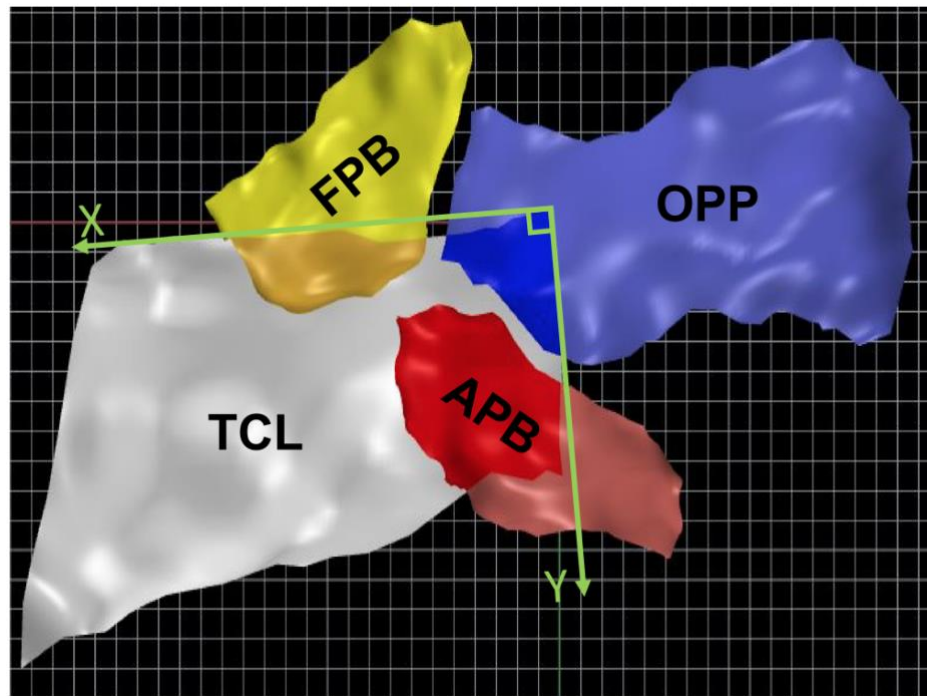


Figure 8. A representative reconstruction of the combined TCL and muscle origin meshes. Bright shades of each color represent origin on the TCL. Dull shades of each color represent origin off the TCL.

Data Analysis: Total surface area for the TCL and muscle origins were calculated. The boundary of the TCL was used to segment each muscle's origin area into the area on

and off the TCL. The origin area on the TCL for each muscle was also normalized by dividing the origin area by total TCL surface area (Figure. 8). The centroids for each muscle origin were also calculated and broken down into their radio-ulnar, proximal-distal, and volar-dorsal components.

Statistical Analysis: All statistical tests were performed in SigmaStat 3.5 (Systat Software Inc, San Jose, CA, USA) with a significance level of 0.05. A two-way repeated measures ANOVA was performed to examine the effect of muscle (APB, FPB, OPP) and origin location (on the TCL, off the TCL) on origin area. A one-way repeated measures ANOVA was also performed to test the effect of muscle on normalized origin area on the TCL. Finally, three one-way repeated measures ANOVAs were performed to examine the effect of muscle on origin centroid in the radioulnar, proximal-distal, volar-dorsal directions. Post-hoc Tukey's tests were performed on all statistical tests to evaluate pairwise comparisons.

3.3 Results

The origin areas for the APB, FPB, and OPP were $105.8 \pm 30.3 \text{ mm}^2$, $64.6 \pm 15.2 \text{ mm}^2$, and $245.9 \pm 70.7 \text{ mm}^2$, respectively, totaling $416.3 \pm 77.9 \text{ mm}^2$ (Figure. 9). Of the three thenar muscles, the origin area of the OPP comprised the largest percent of total thenar area ($58.3 \pm 8.5\%$), followed by the origin area of the APB ($25.8 \pm 7.0\%$) and the origin area of the FPB ($15.9 \pm 4.2\%$).

Origin area was found to significantly differ based on both muscle ($p < 0.001$) and origin location ($p = 0.005$). With respect to muscle, both the OPP ($p < 0.001$) and the FPB ($p = 0.005$) had significantly larger origins off the TCL than origins on the TCL. The APB had a larger origin on the TCL than off the TCL, but the difference in size was not

significant ($p=0.081$). Looking at the location of the muscle origins, the OPP had a significantly larger portion of its origin off the TCL than both the APB and the FPB ($p<0.001$), while the APB and FPB had similarly sized origins off the TCL ($p=0.232$). The APB ($p=0.001$) and OPP ($p=0.003$) both had significantly larger origins located on the TCL than the FPB, but the difference between the origins on the TCL for these two muscles was not significant ($p=0.923$). However, the APB had the largest percentage of its origin fall on the TCL ($68.2\pm16.8\%$) (Figure. 10). Altogether, $34.7\pm15.7\%$ of total thenar area originated from the TCL.

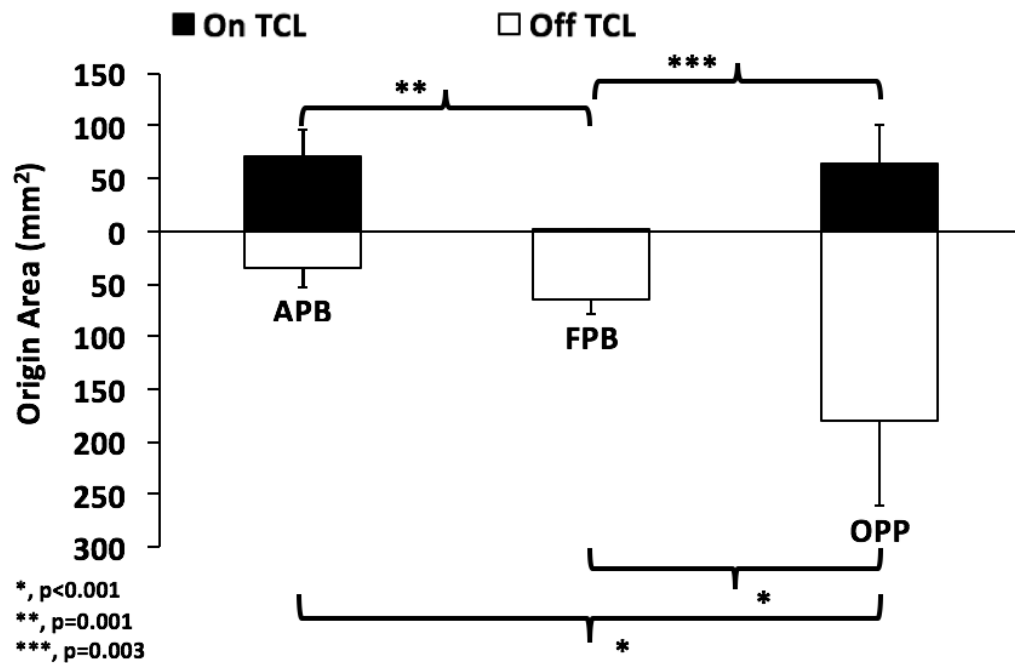


Figure 9. Individual muscle origin areas

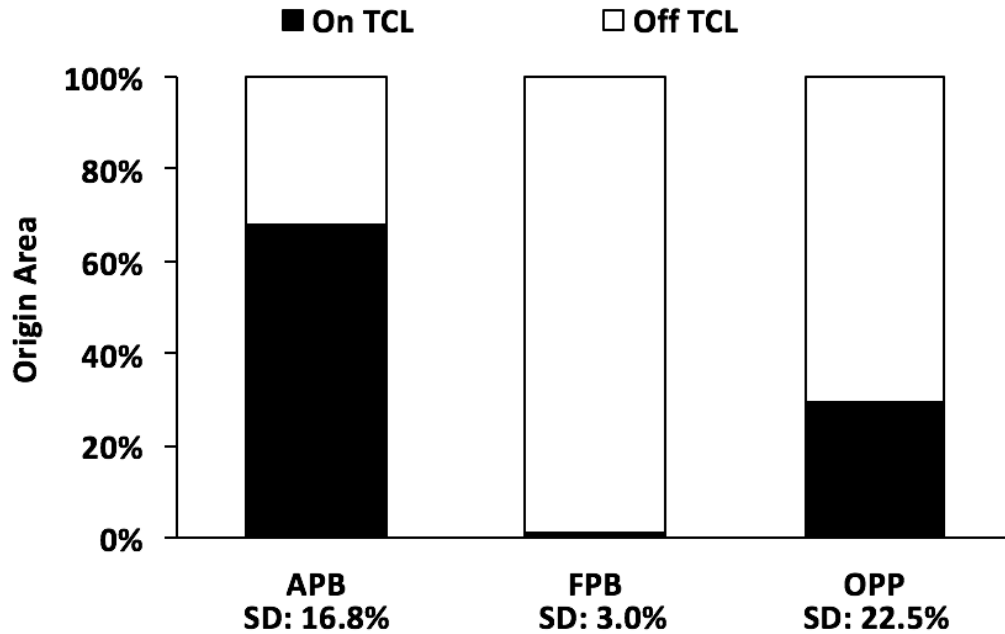


Figure 10. Origin area on and off the TCL normalized by muscle origin area

TCL surface area was $386.2 \pm 86.9 \text{ mm}^2$, of which $137.5 \pm 42.7 \text{ mm}^2$ ($36.0 \pm 10.5\%$) was occupied by the thenar muscles. The contributions of the APB, FPB, and OPP to the muscle area on the TCL were $71.8 \pm 24.5 \text{ mm}^2$, $0.8 \pm 1.8 \text{ mm}^2$, and $64.9 \pm 34.5 \text{ mm}^2$, respectively. The APB, FPB, and OPP occupied $18.4 \pm 4.8\%$, $0.3 \pm 0.6\%$, and $17.3 \pm 9.6\%$ of TCL surface area, respectively (Figure. 11). Significance was found between the muscle origin areas on the TCL with respect to muscle. The FPB occupied significantly less space on the TCL than both the APB ($p < 0.001$) and the OPP ($p < 0.001$). Again, the APB and OPP occupied similar space on the TCL ($p = 0.917$).

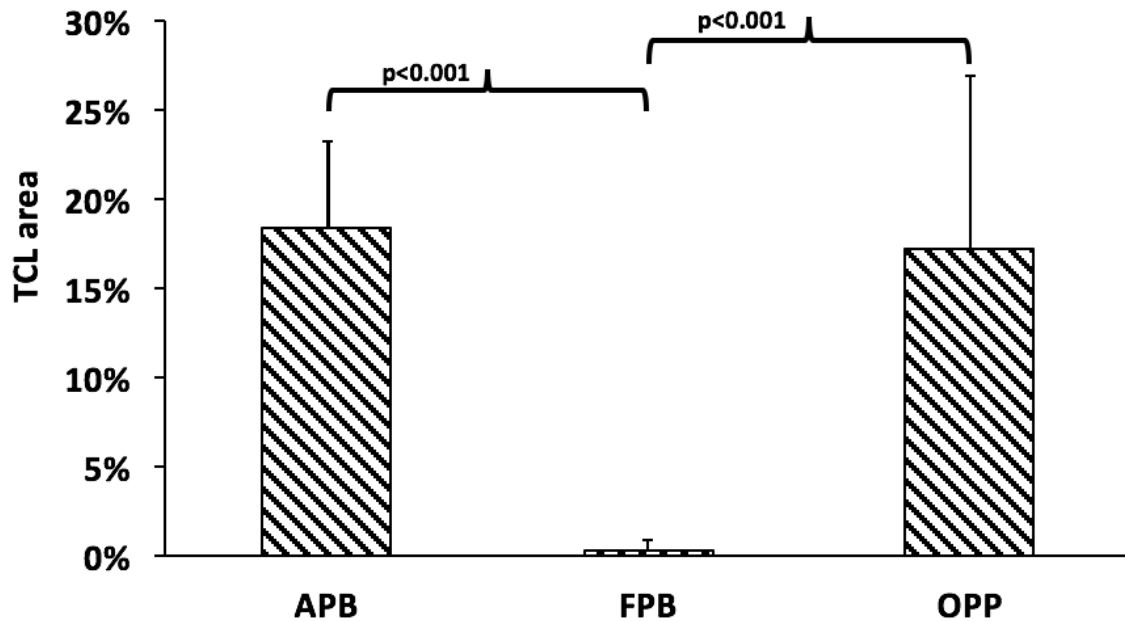


Figure 11. TCL space occupied by each muscle

The muscle origin centroids were significantly affected by the factor of muscle in the radio-ulnar ($p<0.001$), proximal-distal ($p<0.001$), and volar-dorsal ($p=0.004$) directions. With respect to the radio-ulnar direction, all three muscles had significantly different centroid locations ($p<0.001$), with the FPB centroid lying the most ulnar of the three muscles (12.5 ± 3.9 mm from the origin), the centroid of the OPP lying just ulnar to the trapezium (0.3 ± 4.4 mm from the origin), and the APB centroid lying between the other two muscles (7.5 ± 3.3 mm from the origin) (Figure. 12). The proximal-distal locations of each muscle centroid were found to be significantly different ($p<0.001$). In the proximal-distal direction, the APB centroid was the most proximal of the three muscles (7.0 ± 2.9 mm from the origin), with the OPP centroid lying slightly proximal to the trapezium (0.4 ± 1.4 mm from the origin) and the centroid of the FPB lying past the distal end of the TCL (-6.7 ± 2.4 mm from the origin) (Figure. 12). The OPP had a significantly different

volar-dorsal centroid location when compared to the centroids of the APB ($p=0.015$) and FPB ($p=0.006$). The OPP centroid was the most dorsal of the three muscles (-0.3 ± 1.9 mm from the origin) with both the APB (2.4 ± 1.0 mm from the origin) and FPB (2.1 ± 2.2 mm from the origin) lying volar to the OPP. The volar-dorsal centroid locations for the APB and FPB were not significantly different ($p=0.909$).

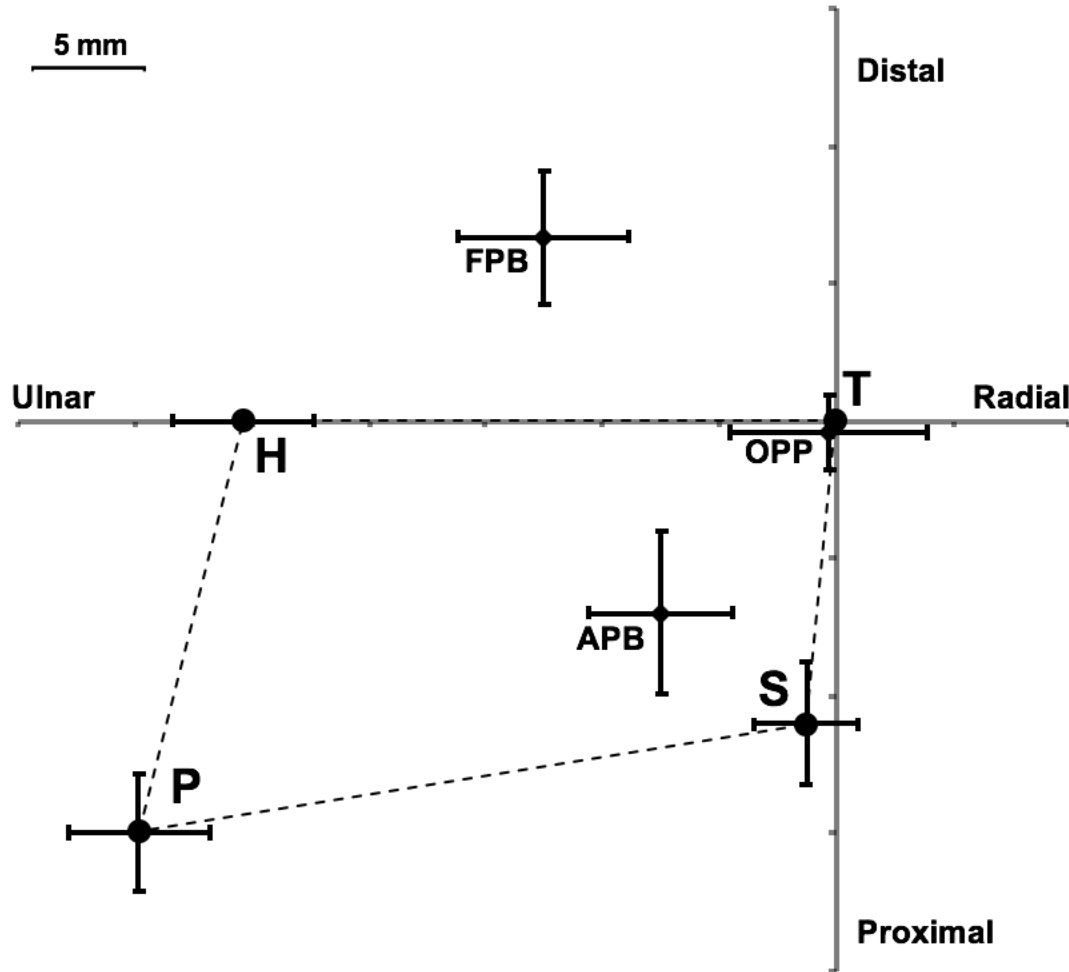


Figure 12. Muscle origin centroid location in the radial-ulnar and proximal-distal directions. H: hamate, T: trapezium, S: scaphoid, P: pisiform

3.4 Discussion

In this study, we quantified the size and location of the individual thenar muscle origins utilizing contact digitization of female cadaveric specimens. Our findings were similar to those reported in previous literature. In a previous study, Kung et al.⁵ quantified the origins of the thenar and hypothenar eminences and reported the mean total thenar muscle origin size to be 530 mm², which was about 100mm² larger than our reported findings. Additionally, Kung et al. reported that 68% of the thenar muscles took origin on the TCL⁵, which was twice as large as our value. Several reasons exist for these differences. Our study utilized all female cadaveric specimens, while the sex of the cadaveric specimens used by Kung et al. was not reported. As well, we used literature unavailable to Kung et al.⁷⁻⁹ to determine the boundaries of the TCL for this study. The TCL boundaries were used to segment each muscle origin into its components on and off the TCL. Kung et al. did not provide a clear definition of the TCL within their study, nor was their method for origin segmentation discussed. Therefore, while Kung et al. provides basic thenar eminence origin information, our study provides a clearer understanding of the individual thenar origins by including the TCL for a complete picture of the relationship between the thenar muscles and TCL.

The evaluation of each muscle's origin size revealed several findings with important implications. Our study found that the OPP had the largest origin size of the three muscles, with the APB having the second largest origin size and the FPB occupying the smallest origin space. A previous study by Fahrer⁵¹ quantified individual muscle origin size and reported similar origin size trends as our results. As well, the OPP had the largest cross-sectional area of the three thenar muscles.⁵⁷ It would be expected that a large origin size

would be necessary to support a large muscle bulk. Additionally, based on the FPB's negligible origin on the TCL, we believe the interactions that the APB and OPP have with the TCL will be greater than the interaction between the FPB and the TCL. Finally, of the three muscles, the APB relied the most on the TCL for its origin. APB muscle contraction may have the greatest effect on the TCL and changes to the TCL may affect the biomechanical function of the APB the most.

Our study also showed that the APB, OPP, and FPB origins were located at three, significantly different locations, which related to each muscle's function. The centroid of the OPP's origin laid just radial and proximal to the trapezium, while the APB originated the most proximally and closest to the center of the TCL and the FPB's origin was the most ulnar and distal. The anatomical location of each muscle, as well as each muscle's function, supports our reported muscle centroid location. The OPP is the most dorsal thenar muscle² and participates mainly in generating pronation of the thumb metacarpal for opposition³, so it is expected that the OPP origin centroid would lie close to the carpometacarpal joint of the thumb. The APB lies above the OPP, so its centroid must lie proximal and ulnar to the OPP centroid. Additionally, the proximal centroid location creates the line-of-action necessary for the APB to generate thumb abduction.³ As for the FPB, flexion of the thumb MCP joint is its main function.² The ulnar and distal origin location maintains the FPB's function regardless of the thumb's current position and does not interfere with the function of the other two muscles. The findings regarding origin location further underscore the relationship between the thenar muscles' anatomical arrangements and their respective function.

Individual thenar muscle origin information may be useful for further exploration of the biomechanical relationship between the thenar muscles and the TCL. Thenar muscle interaction with the TCL have been hypothesized to have implications on the development of CTS and to be altered after surgical interventions for CTS treatment. Based on the noted changes to the TCL's mechanical properties in CTS patients²⁰⁻²² and the TCL's ability to remodel after repetitive mechanical loading^{52,53}, repetitive thenar activation has been suggested as a possible avenue for TCL hypertrophy. Common surgical treatment of CTS includes transection of the TCL, which alters the functional length of the thenar muscles⁴⁹ and may cause reduced pinch strength in CTS patients⁴⁷. Our study provides the deeper understanding of individual thenar muscle anatomy necessary to better explore the above biomechanical phenomena. Specifically, our finding regarding the considerable size of both the APB and OPP origins on the TCL could direct future studies to investigate the consequence of repetitive APB and OPP contraction on the TCL's material properties. Furthermore, the variation among the individual muscle origin centroids may provide the necessary anatomical insight to delve deeper into the consequences of surgical interventions on the individual thenar muscles. Though our study did not investigate the biomechanical relationship between the individual thenar muscles and the TCL, our findings provide the necessary anatomical foundation to further explore the implications of muscle-ligament interaction.

This study is not without limitations. All data for this study was collected using only female cadaveric specimens to eliminate any sex difference. Future studies could follow the procedures developed in this project to determine any sex-based differences in individual thenar muscle origins. Additionally, contact digitization was used for data

collection, which could potentially cause disturbances to the digitized surfaces if too great a pressure was applied and lead to incorrect size and location calculation. Contact digitization is a well-accepted technique for quantification of muscle origins^{5,58} and the TCL⁵⁹. Throughout data collection, light touch of the Microscribe was used to ensure minimal disturbance to the digitized surfaces. The medical balloon within the carpal tunnel provided resistance to excessive digitization pressure while maintaining the shape of the carpal tunnel. Our heavily populated dataset minimized the effects of any possible outliers on the size and location calculations. Future studies could utilize a non-contact digitization approach to reduce the risk of tissue disturbance. In conclusion, this study characterized the individual thenar muscle origins both on and off the TCL.

CHAPTER IV

BIOMECHANICAL INTERACTION BETWEEN THE MUSCLE AND LIGAMENT AFTER TRANSVERSE CARPAL LIGAMENT RELEASE

4.1 Introduction

In addition to anchoring the thenar muscles³, the transverse carpal ligament (TCL) forms the volar border of the carpal tunnel: a fibro-osseous structure housing the median nerve as well as nine flexor tendons. The carpal tunnel relies on the TCL for a multitude of the tunnel's functions, such as providing structural stability to the carpal bones^{11,60}, assisting in the pulley motion of the flexor tendons^{13,14}, and constraining the carpal tunnel contents' volar migration¹². Changes to the tunnel's compliance or a reduction in carpal tunnel space can compress the median nerve and lead to the development of Carpal Tunnel Syndrome (CTS). CTS is the most common median nerve neuropathy, affecting between 3-5% of the general population^{17,18} and causes numbness, pain, and loss of sensation in the median nerve innervated digits¹⁹.

A prevalent surgical intervention for CTS treatment is carpal tunnel release (CTR) surgery, where an average of 450,000 CTR surgeries are performed annually in the US, costing in excess of 2 billion dollars.²⁹ During CTR, the TCL is partially or completely transected to increase carpal tunnel volume and reduce carpal tunnel pressure. Patients

with mild or moderate CTS symptoms who undergo CTR report significant symptom relief after release.³⁰ However, an array of surgical complications, such as incomplete TCL release³² and median nerve fibrosis⁴¹, arise post-surgery. Moreover, the extent to which TCL transection disrupts the carpal tunnel's biomechanics is still being investigated.⁶¹ The contact forces between the carpal bones and their location are altered after release^{44,45}, affecting the carpal tunnel's overall structure. Transection of the TCL drastically reduces the TCL's ability to restrict the volar migration of the flexor tendons, increasing the frequency of trigger finger in CTR patients⁴⁸ and decreasing pinch and grip strengths postoperatively^{46,47}.

Altered thenar muscle interaction with the TCL after release is another biomechanical consequence of surgery that has not been explored. Kung et al.⁵ showed that 68% of thenar muscle attachments lie on the TCL, and the thenar muscles rely on their TCL anchoring to generate thumb force production¹. Transection of the TCL does alter the effective length of the thenar muscles⁴⁹, which may in turn alter the biomechanical interaction between the thenar muscles and the TCL. This altered interaction may potentially explain the decreased grip strength seen in surgically repaired hands.⁴³ Further information regarding muscle-ligament interaction after TCL release may provide insight into the cause of reduced hand strength post-operatively and provide a direction for new surgical procedures with reduced biomechanical impact. Therefore, the purpose of this study was to examine the effect of TCL release on muscle-ligament interaction. We quantified the effect of TCL release by measuring the morphological parameters in the TCL-formed carpal arch before and after thenar muscle loading in

intact and released cadaveric specimens. We hypothesized that carpal arch height, width, and area will be significantly affected by TCL release.

4.2 Methods

Specimens: Eight freshly-frozen male cadaveric specimens (right hands; mean age 53.5 ± 13.2 years; mean BMI 25.0 ± 4.0) were used in this study. Specimens with histories of hand or wrist musculoskeletal disorder or injury were excluded from this study.

Dissection: Prior to dissection, each specimen was removed from a storage freezer and thawed for at least 12 hours to room temperature. For each specimen, the skin and fat above the thenar muscles were dissected following the white path shown in Figure. 13 and reflected towards the ulnar side of the hand for visualization of the thenar muscles. The APB muscle body was separated from the rest of the thenar muscles, and the tendinous insertion of APB was dissected. Similarly, the FPB was separated from the OPP, the FPB's tendinous insertion was dissected, and the FPB's superficial head was separated from the deep head. Next, a first metacarpal osteotomy was performed so the OPP's bony insertion could be separated from the rest of the metacarpal for loading (Figure. 14). Using the Krackow stitch method, surgical sutures were secured through the tendinous insertions of the APB and superficial head of the FPB for muscle loading. A clamp was attached to the partial thumb metacarpal for loading of the OPP (Figure. 14). Incisions were made above the distal ends of the radius, ulna, 2nd, and 4th metacarpals in preparation for securing the specimen. During dissection, great care was taken to maintain the integrity of the soft tissues above the TCL.

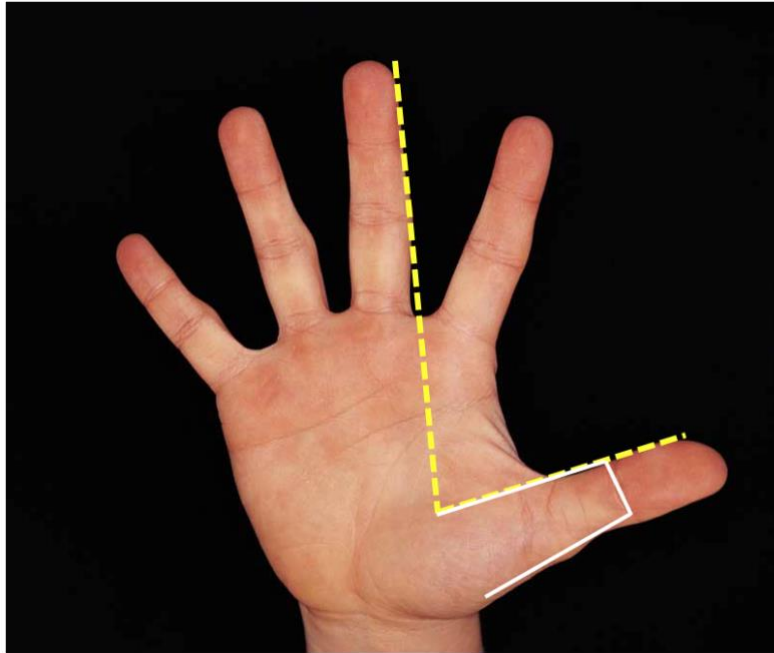


Figure 13. Incision path for dissection. Dotted yellow lines were used to direct the path of incision (white).

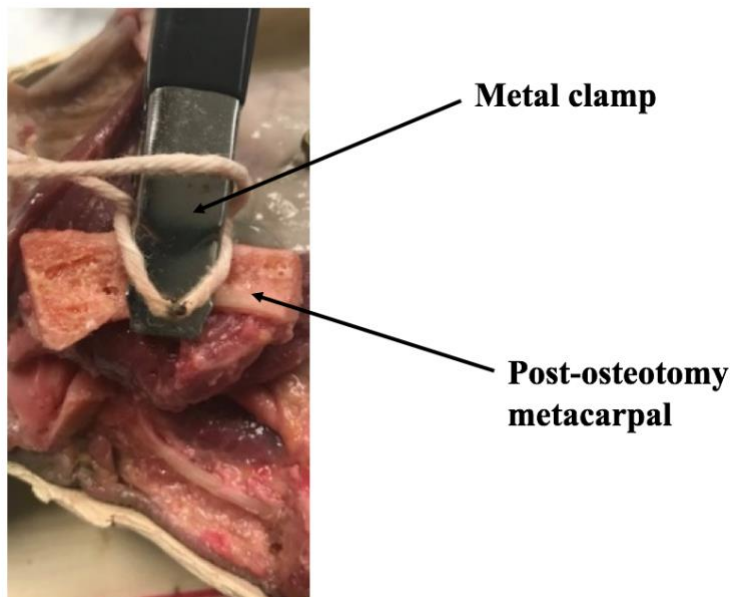


Figure 14. Post osteotomy clamping of the first metacarpal used for OPP loading

Experimental Apparatus: A custom-made apparatus was designed to assist in thenar muscle loading (Figure. 15). Three, separate pulley systems were attached to a wooden block. Each pulley system interacted with one muscle and could be adjusted to properly direct muscle loading. An ultrasound holder was attached on top of the wooden block for securing the ultrasound probe during testing.

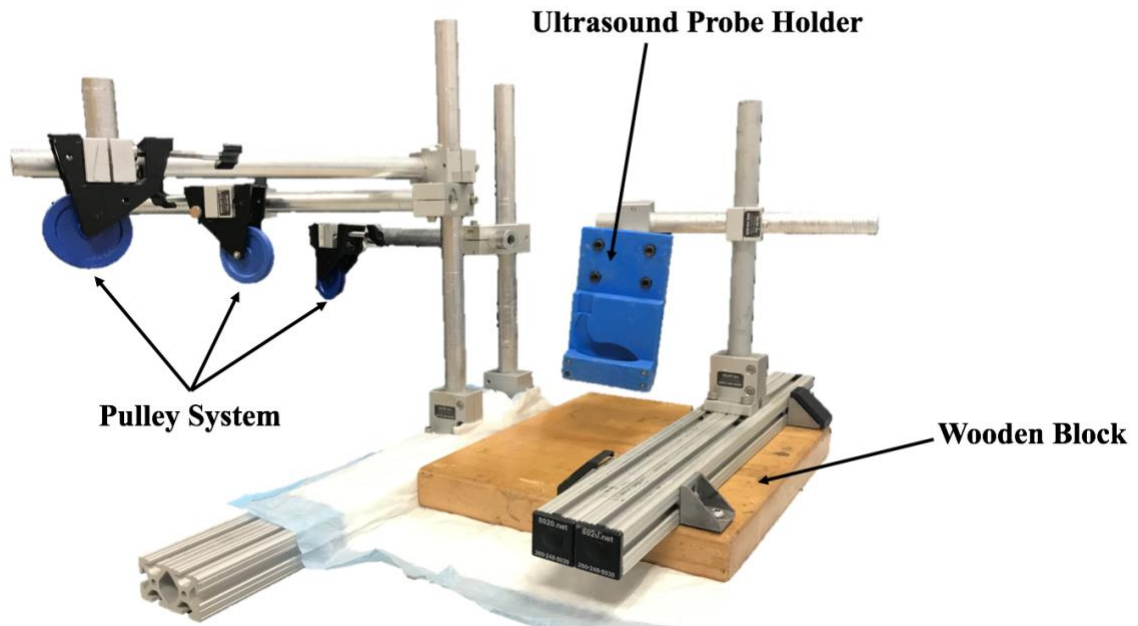


Figure 15. Experimental set-up for thenar muscle loading

Experimental Setup: Each specimen was placed supine in a thermoplastic splint, the thumb was positioned in an abducted and pronated position similar to pinching, and the fingers were oriented in a neutral position. Velcro straps were used to secure the specimen's forearm, fingers, and thumb. The specimen and splint were placed on top of a wooden board and secured to the board using screws drilled through the incisions above the radius, ulna, and metacarpals (Figure. 16). During this step, the tendons above the bones were bypassed in order to minimize the effect of drilling on the carpal tunnel

contents. The board was then affixed to the wooden block of the apparatus. The free ends of each muscle's suture were passed across the corresponding pulley. The height and orientation of the pulley was adjusted according to the anatomical orientation of each muscle's fiber direction for optimal muscle loading (Figure. 16). An 18L6 HD linear array probe (Acuson S2000, Siemens Medical Solutions USA, Mountain View, CA) was secured in the ultrasound probe holder above the wrist at the distal carpal tunnel and fixed at that position. The ultrasound probe was connected to an ultrasound system (Acuson S2000, Siemens Medical Solutions USA, Mountain View, CA) for recording distal TCL morphological change during the experiment. The loading magnitude for each muscle was determined as 15% of its maximal muscle force production as reported in the literature⁶² (Table. 1). Muscle loading was generated by adding sand-filled containers to the free ends of the muscle sutures.

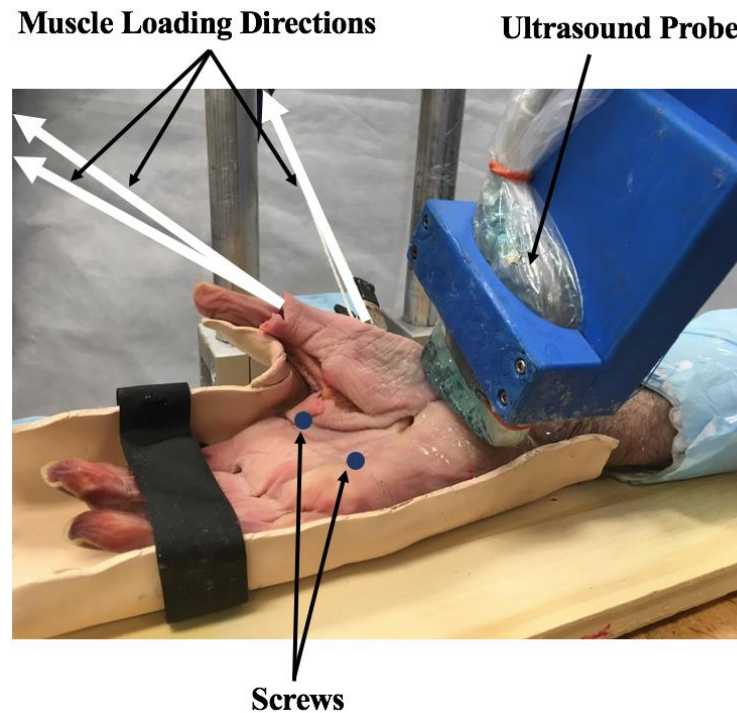


Figure 16. Specimen secured in experimental apparatus

Table I. Selected loading magnitudes for individual thenar muscles

	15% Maximum force (N)	15% Maximum force (kg)
APB	8.09	0.83
FPB	4.78	0.49
OPP	13.98	1.43

Experimental Protocol: During experimentation, seven loading conditions (APB, FPB, OPP, APB-FPB, FPB-OPP, APB-OPP, and ALL) were applied to the muscles in a randomized order. Three trials of each loading condition were collected, totaling 21 trials. A 30 second ultrasound video was collected at 30 frames per second for each trial, consisting of 5 seconds of the specimen unloaded followed by 25 seconds of the specimen loaded. After each trial, the muscles were unloaded and 30 seconds of rest were given for the muscles to relax. Throughout data collection, ultrasound videos were collected in two-dimensional B-mode within a frequency range of 8 to 12 MHz, a gain of 8 dB, and an image depth between 2-4 cm. After collecting the videos for the intact trials, each specimen underwent endoscopic carpal tunnel release performed by a trained hand surgeon using an endoscopic release device (SmartRelease, MicroAire, Charlottesville, VA, USA). Endoscopic release was selected as it maintained the integrity of the tissues volar to the TCL. Multiple passes of the release device ensured complete release of the TCL. After TCL release, the specimens were secured back on the wooden block and the same experimental protocol was performed to collect released trials of muscle loading. When testing was completed, each specimen was volarly dissected to ensure complete TCL release.

Data Processing and Analysis: Morphological changes of the carpal tunnel were quantified by measuring three carpal arch parameters within each video: carpal arch width (CAW), carpal arch height (CAH), and carpal arch area (CAA). For both the intact and released trials, the ultrasound videos for each trial were separated into a collection of ultrasound frames. The 50th frame (middle of the first 100 frames) and 850th (middle of the last 100 frames) frame were selected to represent the specimen when it was unloaded and loaded, respectively. Using a custom LabVIEW code, the hamate, trapezium, and volar border of the TCL were manually traced in both frames. CAW was defined as the distance between the hamate and the trapezium. CAH was determined as the greatest perpendicular distance between the traced TCL and the CAW. CAA was calculated using the polygon formed by all traced points (Figure. 17). CAW, CAH, and CAA calculated in the 50th frame represented the unloaded carpal arch parameters, and the CAW, CAH, and CAA calculated in the 850th frame represented the loaded carpal arch parameters. For both the intact and released trials, the carpal arch parameters were normalized by subtracting the unloaded carpal arch parameters from loaded carpal arch parameters within the same trial.

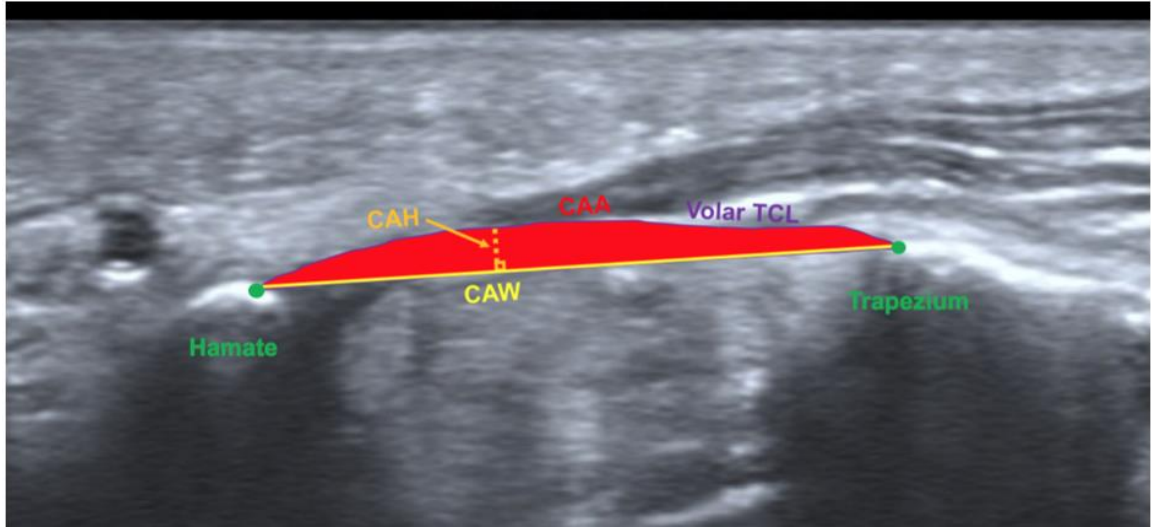


Figure 17. Quantification of carpal arch height, width, and area from traced hamate, trapezium, and volar TCL border

Statistical Analysis: SigmaStat 3.5 (Systat Software Inc, San Jose, CA, USA) was used to run statistical tests on all the data. A one-way, repeated measures ANOVA was performed on unloaded CAW for the intact and released specimens to examine the expected change in CAW after TCL release. Two-way, repeated-measures ANOVA were performed to examine the influence of loading condition (APB, FPB, OPP, APB-FPB, APB-OPP, FPB-OPP, ALL) and TCL status (intact, released) on the normalized carpal arch parameters (CAH, CAW, and CAA). Post hoc Tukey's tests were used for all pairwise comparisons with a significance level of 0.05.

4.3 Results

Volar dissection of all eight specimens after data collection showed complete release of the distal TCL. Successful release of all specimen was further supported by our finding that unloaded CAW after release (26.1 ± 2.5 mm) was significantly larger than unloaded CAW before release (24.8 ± 2.2 mm) ($p=0.024$).

Figures. 18, 19, and 20 show the normalized CAH, CAW, and CAA, respectively, for both the intact and released specimens. With respect to normalized CAH, condition ($p=0.17$), TCL status ($p=0.24$), and the interaction between condition and TCL status ($p=0.14$) did not significantly affect normalized CAH, though the individual muscle loading conditions showed a reduction in their normalized CAH after CTR (APB: 0.16 ± 0.23 mm before release vs. 0.05 ± 0.27 mm after release, FPB: 0.11 ± 0.10 mm before release vs. 0.09 ± 0.12 mm after release, OPP: -0.13 ± 0.32 mm before release vs. -0.08 ± 0.34 mm after release) (Figure. 18). Normalized CAW was not significantly affected by TCL status ($p=0.97$) or the interactions between condition and TCL status ($p=0.157$), but loading condition did significantly affect normalized CAW ($p=0.018$). It was found that the OPP generated greater changes in CAW during muscle loading than the FPB within the intact specimens ($p=0.008$), but no significant difference was found between the two loading conditions in the released specimens ($p=0.422$). Again, the trend of normalized CAW in the individual muscle loading conditions was altered after CTR (APB: -0.16 ± 0.71 mm before release vs. 0.13 ± 0.42 mm after release, FPB: -0.32 ± 0.52 mm before release vs. 0.00 ± 0.42 mm after release, OPP: 0.58 ± 0.48 mm before release vs. 0.50 ± 0.57 mm after release) (Figure. 19). Condition ($p=0.21$), TCL status ($p=0.24$), and the interaction between condition and TCL status ($p=0.94$) were all found to not have significant effects on normalized CAA, though the trend in normalized CAA for the individual muscle loading conditions was altered after CTR (APB: 3.9 ± 2.7 mm² before release vs. 0.70 ± 7.1 mm² after release, FPB: 0.86 ± 1.1 mm² before release vs. -0.83 ± 2.4 mm² after release, OPP: 1.2 ± 4.1 mm² before release vs. -2.4 ± 7.8 mm² after release) (Figure. 20).

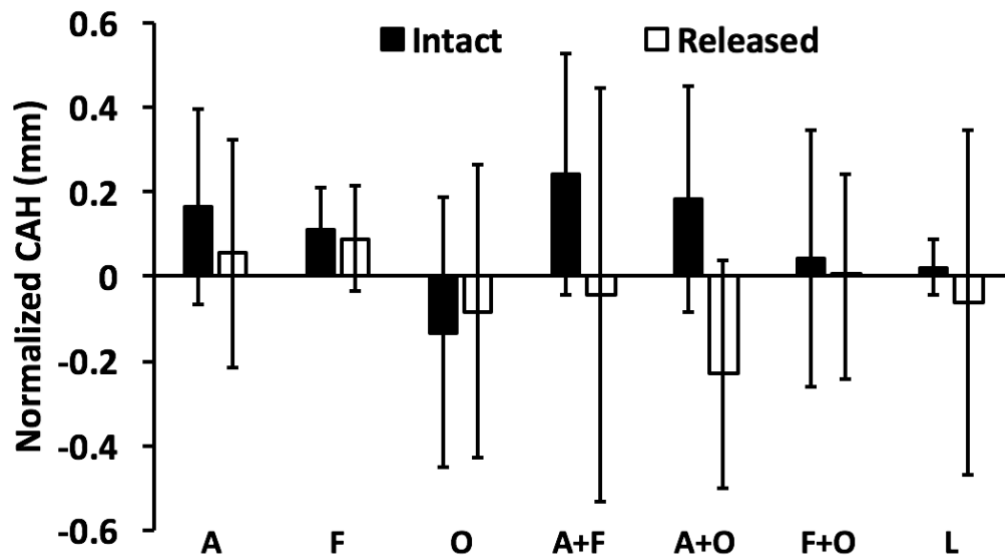


Figure 18. Normalized CAH for the intact and released trials. A: APB, F: FPB, O: OPP, A+F: APB-FPB, A+O: APB-OPP, F+O: FPB-OPP, L: ALL

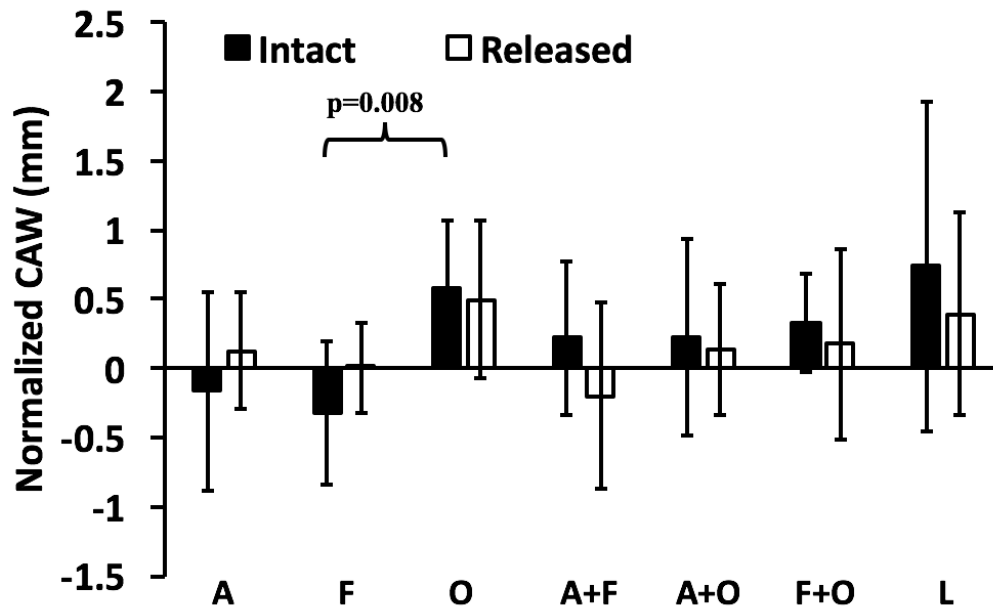


Figure 19. Normalized CAW for the intact and released trials. A: APB, F: FPB, O: OPP, A+F: APB-FPB, A+O: APB-OPP, F+O: FPB-OPP, L: ALL

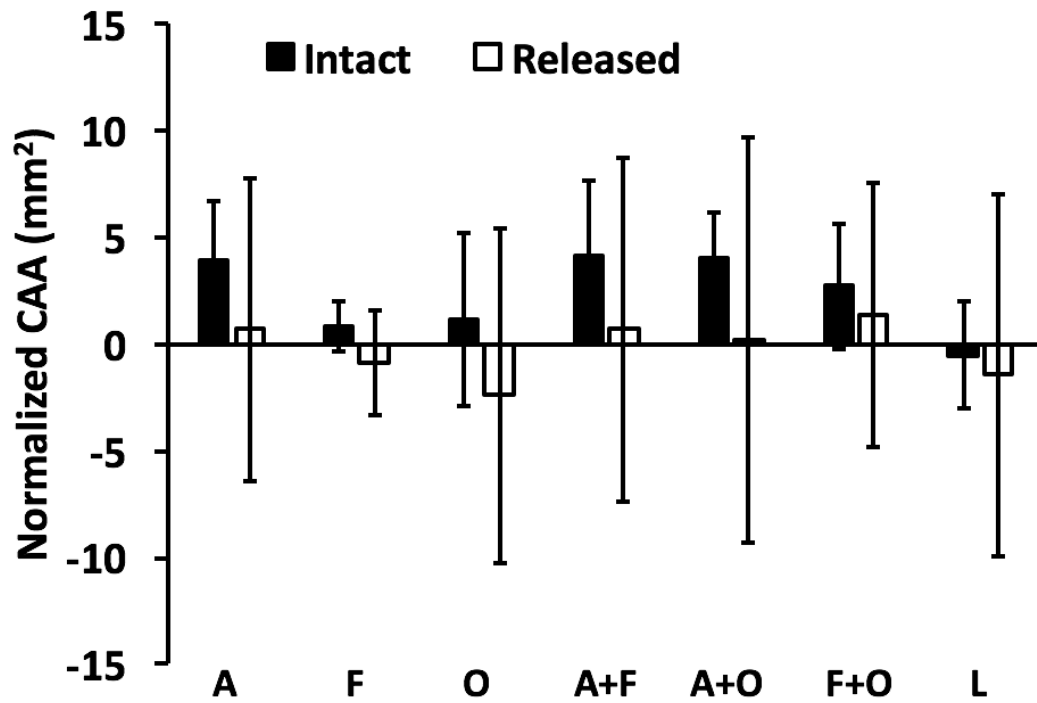


Figure 20. Normalized CAA for the intact and released trials. A: APB, F: FPB, O: OPP, A+F: APB-FPB, A+O: APB-OPP, F+O: FPB-OPP, L: ALL

4.4 Discussion

This study utilized endoscopic carpal tunnel release for TCL transection. Endoscopic carpal tunnel release has been shown to increase carpal arch width between 7%-11% on average^{63,64}, with 70% of cases showing an increase of only 0-10%⁶³. In our study, we found an average CAW increase of 5.2% after release, which falls within the previously reported range. This finding, in addition to our visual inspection of complete distal TCL release for all eight specimens, affirms the success of our endoscopic release procedure in achieving accurate TCL release. Moreover, quantification of a significant increase in CAW after endoscopic CTR supports our ability to detect small changes in carpal arch morphology using our manual processing algorithm.

One possibility for the lack of significant findings within our study was the inconsistent relationship between the location of TCL transection and the thenar muscle origins across specimens. Such inconsistency might lead to the varied biomechanical response of the carpal arch during thenar muscle loading seen in the specimens, resulting in a lack of distinguishable pattern within the normalized carpal arch parameters. Specifically, during endoscopic carpal tunnel release, the path of TCL transection was determined by a line passing through the third web space of the hand and the distal wrist crease, as described in the literature²⁶. Though the use of ulnar surface landmarks to direct transection ensured no damage to the radial structures in the specimens, the transection location was determined without consideration for the locations of the thenar muscle origins. In Aim 1, we reported three, distinct locations for the muscle origin centroids of the APB, FPB, and OPP. However, we found high variability in origin location across specimens, reflected by the substantial standard deviations for the radio-ulnar and proximal-distal centroid locations. As well, previous literature has reported high incidence of musculature crossing the path of TCL transection.^{39,40} Therefore, it is possible that the relationship between the thenar muscle origins and the location of TCL transection was not consistent across specimens. The individual muscle-ligament biomechanical interaction may differ based on whether the TCL transection was radial, ulnar, or through the muscle origin. Future studies may use an imaging modality, such as ultrasound, to direct endoscopic carpal tunnel release to maintain a consistent relationship between the transection location and the muscle origins.

The unknown mechanical function of the tissues volar to the TCL may have also played a role in our inconclusive findings. Morell et al.⁶¹ explored the biomechanical

consequences of CTR and noted that increases in carpal arch width reported after open release (13.6% average 19.7 months post-CTR in Gartsman et al.⁶⁵) were larger than the increases reported after endoscopic release (7% average in Veigas et al.⁶³, 11% average in Garcias-Elias et al.⁶⁴). The authors suggested that the role of the tissues volar to the TCL, specifically the skin, play an unknown role in support of the carpal tunnel.⁶¹ It is possible that the skin and superficial tissues above the TCL interfered with muscle loading once the TCL was released. A future study may investigate the role of the superficial tissues with respect to TCL function.

The lack of intratunnel pressure within the specimens could have affected our results. Because the TCL stabilizes the carpal tunnel¹¹ and constraints the carpal tunnel contents¹², the TCL is naturally under tension. Once the TCL is released, no tension remains in the TCL and the TCL will sag without any intratunnel pressure to maintain the arch shape. Indeed, a previous study⁶⁶ that investigated the effect of pressure on the released TCL in cadaveric specimens discarded the data between 0 and 10 mmHg based on the concavity of the TCL directly after release. Reduced concavity of the TCL could lead to unexpected and insignificant responses to mechanical loading when the thenar muscles were loaded. We chose not to insert a medical balloon or other pressure-maintaining device within the carpal tunnel of each specimen to maintain the integrity of the TCL and carpal tunnel contents after release. Future studies could follow our given methods with the addition of a medical balloon inside the carpal tunnel to mitigate this possible roadblock.

Finally, our lack of conclusive findings may have spawned from the low loading magnitude selected for this experiment. Fifteen percent of maximum muscle contractile

force was selected because higher loading magnitudes caused failure of the individual thenar muscles during testing. Cadaveric tissues lack the capacity to generate active contraction of the individual thenar muscles, so our biomechanical testing had to rely on the passive properties of the cadaveric muscle tissues to sustain loading. Based on the deficiencies of cadaveric specimen with respect to muscle loading, future studies should utilize living subjects with voluntary muscle contraction to explore CTR's biomechanical consequence on muscle-ligament interaction.

Carpal tunnel release is a common surgical intervention for treating CTS²⁹ and has been shown to relieve some symptoms³¹. However, TCL transection is known to decrease the stability of the carpal bones^{44,45}, increase carpal tunnel compliance³⁴, reduce the TCL's assistance in flexor tendon function^{47,48}, and alter the effective contractile length of the thenar muscles⁴⁹. Though we were unable to prove our hypothesis regarding the biomechanical consequence of TCL release, our data suggests that TCL release may have some effect on muscle-ligament interaction. Future studies should continue to explore muscle-ligament interaction after TCL release to fully illuminate this possible biomechanical consequence of CTR. The proposed alternatives to our performed method can be used to design a future cadaveric study that reduces the number of confounding variables. Additionally, utilizing living subjects with voluntary or involuntary thenar muscle contraction may provide a deeper understanding of the biomechanical consequence of TCL transection.

This study was not without limitation. Only male specimens were used in this study. Future studies may investigate the biomechanical influence of TCL release on muscle-ligament interaction within females or across sexes. Despite the inconclusive findings, this

study implies that the interaction between the thenar muscles and TCL after TCL transection is a complicated process which is influenced by both anatomical and surgical variations not considered in this project. Future studies with reduced confounding variables are needed to get a conclusive answer.

CHAPTER V

CONCLUSIONS

In this study, we utilized dissection and mechanical testing of cadaveric specimens to investigate the anatomical and biomechanical relationships between the thenar muscles and the TCL. We characterized each muscle's distinct origin size and location both on and off the TCL, noting that the OPP had the largest area of origin and APB had the most proximal origin centroid location on the TCL. We observed the APB's reliance on the TCL for its origin while both the OPP and FPB originate mainly from the tissue surrounding the TCL. We also observed altered patterns of the muscle-ligament interaction after the TCL was released, though these observations remain inconclusive. The observations within this thesis indicate that each thenar muscle has a distinct anatomical relationship with the TCL and that muscle-ligament interaction is a complex biomechanical phenomenon. Additional knowledge regarding the factors influencing muscle-ligament interaction may help illuminate the exact cause of altered interaction after CTR. Surgical intervention for CTS treatment could potentially be revised to reduce the changes in normal hand biomechanics if the factors influencing muscle-ligament interaction are better understood. This thesis provides the necessary anatomical and

biomechanical foundation to further explore the relationship between the thenar muscles and the TCL.

REFERENCES

1. Imaeda T, An K, Cooney 3rd W. functional anatomy and biomechanics of the thumb. *Hand Clin.* 1992.
2. Botte MJ. Muscle anatomy. In: Doyle JR, Botte MJ, eds. *Surgical Anatomy of the Hand and Upper Extremity*. Lippincott Williams & Wilkins; 2003:149-154.
3. Gupta S, Michelsen-Jost H. Anatomy and function of the thenar muscles. *Hand Clin.* 2012. doi:10.1016/j.hcl.2011.09.006
4. Leversedge FJ. Anatomy and Pathomechanics of the Thumb. *Hand Clin.* 2008. doi:10.1016/j.hcl.2008.03.010
5. Kung J, Budoff JE, Wei ML, Gharbaoui I, Luo ZP. The origins of the thenar and hypothenar muscles. *J Hand Surg Am.* 2005. doi:10.1016/j.jhsb.2005.04.019
6. Cobb TK, Dalley BK, Posteraro RH, Lewis RC. Anatomy of the flexor retinaculum. *J Hand Surg Am.* 1993. doi:10.1016/0363-5023(93)90251-W
7. Goitz R, Fowler J, LI Z-M. The Transverse Carpal Ligament: Anatomy and Clinical Implications. *J Wrist Surg.* 2014. doi:10.1055/s-0034-1394150
8. Stecco C, Macchi V, Lancerotto L, Tiengo C, Porzionato A, De Caro R. Comparison of Transverse Carpal Ligament and Flexor Retinaculum Terminology for the Wrist. *J Hand Surg Am.* 2010. doi:10.1016/j.jhsa.2010.01.031
9. Manley M, Boardman M, Goitz RJ. The carpal insertions of the transverse carpal ligament. *J Hand Surg Am.* 2013. doi:10.1016/j.jhsa.2013.01.015
10. Li Z-M, Marquardt T, Evans P, Seitz W. Biomechanical Role of the Transverse Carpal Ligament in Carpal Tunnel Compliance. *J Wrist Surg.* 2014. doi:10.1055/s-0034-1394136

11. Xiu KH, Kim JH, Li ZM. Biomechanics of the transverse carpal arch under carpal bone loading. *Clin Biomech.* 2010. doi:10.1016/j.clinbiomech.2010.05.011
12. Netscher D, Lee M, Thornby J, Polsen C. The effect of division of the transverse carpal ligament on flexor tendon excursion. *J Hand Surg Am.* 1997. doi:10.1016/S0363-5023(97)80041-X
13. Kline SC, Moore JR. The transverse carpal ligament. An important component of the digital flexor pulley system. *J Bone Jt Surg - Ser A.* 1992. doi:10.2106/00004623-199274100-00006
14. Levangie PK, Norkin CC. The Wrist and Hand Complex. In: Levangie PK, Norkin CC, eds. *Joint Structure and Function: A Comprehensive Analysis.* 5th ed. Philadelphia: F.A. Davis Company; 2011:315-319.
15. Shen ZL, Li Z-M. Biomechanical interaction between the transverse carpal ligament and the thenar muscles. *J Appl Physiol.* 2012. doi:10.1152/japplphysiol.01273.2012
16. Selvaraj N. Biomechanics of Thenar Muscles and Transverse Carpal Ligament During Pipetting. 2018. http://rave.ohiolink.edu/etdc/view?acc_num=csu1528985532616584.
17. Atroshi I, Gummesson C, Johnsson R, Ornstein E, Ranstam J, Rosén I. Prevalence of carpal tunnel syndrome in a general population. *J Am Med Assoc.* 1999. doi:10.1001/jama.282.2.153
18. Ibrahim I, Khan W., Goddard N, Smitham P. Carpal Tunnel Syndrome: A Review of the Recent Literature. *Open Orthop J.* 2012. doi:10.2174/1874325001206010069

19. Zyluk A, Kosovets L. An assessment of the sympathetic function within the hand in patients with carpal tunnel syndrome. *J Hand Surg Eur Vol.* 2010.
doi:10.1177/1753193410361292
20. John V, Nau HE, Nahser HC, Reinhardt V, Venjakob K. CT of carpal tunnel syndrome. *Am J Neuroradiol.* 1983.
21. Yamagami T, Higashi K, Handa H, et al. Carpal tunnel syndrome: Clinical experience of 61 cases. *Neurol Surg.* 1994.
22. T.L. M, J.N. G, P.J. E, W.H. S. Thickness and stiffness changes of the transverse carpal ligament in carpal tunnel syndrome patients. *J Orthop Res.* 2016.
doi:http://dx.doi.org/10.1002/jor.23247
23. Schuind F, Ventura M, Pasteels JL. Idiopathic carpal tunnel syndrome: Histologic study of flexor tendon synovium. *J Hand Surg Am.* 1990. doi:10.1016/0363-5023(90)90070-8
24. Huisstede BM, Hoogvliet P, Randsdorp MS, Glerum S, van Middelkoop M, Koes BW. Carpal Tunnel Syndrome. Part I: Effectiveness of Nonsurgical Treatments—A Systematic Review. *Arch Phys Med Rehabil.* 2010.
doi:10.1016/j.apmr.2010.03.022
25. Rojo-Manaute JM, Capa-Grasa A, Chana-Rodríguez F, et al. Ultra-minimally invasive ultrasound-guided carpal tunnel release: A randomized clinical trial. *J Ultrasound Med.* 2016. doi:10.7863/ultra.15.07001
26. Chow JCY. Endoscopic release of the carpal ligament for carpal tunnel syndrome: 22-month clinical result. *Arthrosc J Arthrosc Relat Surg.* 1990. doi:10.1016/0749-8063(90)90058-L

27. Jakab E, Ganos D, Cook FW. Transverse carpal ligament reconstruction in surgery for carpal tunnel syndrome: A new technique. *J Hand Surg Am.* 1991.
doi:10.1016/S0363-5023(10)80097-8
28. Seitz WH, Lall A. Open carpal tunnel release with median neurolysis and Z-plasty reconstruction of the transverse carpal ligament. *Curr Orthop Pract.* 2013.
doi:10.1097/BCO.0b013e3182797ac3
29. Falkiner S, Myers S. When exactly can carpal tunnel syndrome be considered work-related? *ANZ J Surg.* 2002. doi:10.1046/j.1445-2197.2002.02347.x
30. Bland JDP. Carpal tunnel syndrome. *BMJ.* 2007;335(7615):343-346.
doi:10.1136/bmj.39282.623553.AD
31. Shi Q, MacDermid JC. Is surgical intervention more effective than non-surgical treatment for carpal tunnel syndrome? a systematic review. *J Orthop Surg Res.* 2011. doi:10.1186/1749-799X-6-17
32. Einhorn N, Leddy JP. Pitfalls of endoscopic carpal tunnel release. *Orthop Clin North Am.* 1996.
33. Yoshida A, Okutsu I, Hamanaka I. Is complete release of all volar carpal canal structures necessary for complete decompression in endoscopic carpal tunnel release? *J Hand Surg Eur Vol.* 2007. doi:10.1016/j.jhse.2007.04.002
34. Ratnaparkhi R, Xiu K, Guo X, Li ZM. Changes in carpal tunnel compliance with incremental flexor retinaculum release. *J Orthop Surg Res.* 2016.
doi:10.1186/s13018-016-0380-3
35. Varitimidis SE, Herndon JH, Sotereanos DG. Failed endoscopic carpal tunnel release. Operative findings and results of open revision surgery. *J Hand Surg Am.*

1999. doi:10.1054/jhsb.1999.0243
36. Hurwitz PJ. Variations in the Course of the Thenar Motor Branch of the Median Nerve. *J Hand Surg (British Eur Vol.* 1996. doi:10.1016/S0266-7681(05)80198-6
 37. Green DP, Morgan JP. Correlation Between Muscle Morphology of the Transverse Carpal Ligament and Branching Pattern of the Motor Branch of Median Nerve. *J Hand Surg Am.* 2008. doi:10.1016/j.jhsa.2008.05.025
 38. Al-Qattan MM. Variations in the course of the thenar motor branch of the median nerve and their relationship to the hypertrophic muscle overlying the transverse carpal ligament. *J Hand Surg Am.* 2010. doi:10.1016/j.jhsa.2010.08.011
 39. Hollevoet N, Barbaix E, D'Herde K, Vanhove W, Verdonk R. Muscle fibres crossing the line of incision used in carpal tunnel decompression. *J Hand Surg Eur Vol.* 2010. doi:10.1177/1753193409102465
 40. Jegal M, Woo SJ, Lee H Il, Shim JW, Shin WJ, Park MJ. Anatomical relationships between muscles overlying distal transverse carpal ligament and Thenar motor branch of the median nerve. *CiOS Clin Orthop Surg.* 2018. doi:10.4055/cios.2018.10.1.89
 41. Stütz NM, Gohritz A, van Schoonhoven J, Lanz U. Revision surgery after carpal tunnel release - Analysis of the pathology in 200 cases during a 2 year period. *J Hand Surg Am.* 2006. doi:10.1016/j.jhsb.2005.09.022
 42. Nancollas MP, Peimer CA, Wheeler DR, Sherwin FS. Long-term results of carpal tunnel release. *J Hand Surg Am.* 1995. doi:10.1016/S0266-7681(05)80155-X
 43. Brooks JJ, Schiller JR, Allen SD, Akelman E. Biomechanical and anatomical consequences of carpal tunnel release. *Clin Biomech.* 2003. doi:10.1016/S0268-

0033(03)00052-4

44. Schiller J, Brooks J, Mansuripur P, Gil J, Akelman E. Three-Dimensional Carpal Kinematics after Carpal Tunnel Release. *J Wrist Surg.* 2016. doi:10.1055/s-0036-1578812
45. Guo X, Fan Y, Li ZM. Effects of dividing the transverse carpal ligament on the mechanical behavior of the carpal bones under axial compressive load: A finite element study. *Med Eng Phys.* 2009. doi:10.1016/j.medengphy.2008.08.001
46. Gellman H, Kan D, Gee V, Kuschner SH, Botte MJ. Analysis of pinch and grip strength after carpal tunnel release. *J Hand Surg Am.* 1989. doi:10.1016/S0363-5023(89)80091-7
47. Mathur K, Pynsent PB, Vohra SB, Thomas B, Deshmukh SC. Effect of wrist position on power grip and key pinch strength following carpal tunnel decompression. *J Hand Surg Am.* 2004. doi:10.1016/j.jhsb.2004.02.012
48. Lee SK, Bae KW, Choy WS. The relationship of trigger finger and flexor tendon volar migration after carpal tunnel release. *J Hand Surg Eur Vol.* 2014. doi:10.1177/1753193413479506
49. Fuss FK, Wagner TF. Biomechanical alterations in the carpal arch and hand muscles after carpal tunnel release: A further approach toward understanding the function of the flexor retinaculum and the cause of postoperative grip weakness. *Clin Anat.* 1996;9:100-108. doi:10.1002/(sici)1098-2353(1996)9:2<100::aid-ca2>3.0.co;2-l
50. McFarlane RM. Observations on the Functional Anatomy of the Intrinsic Muscles of the Thumb. *J Bone Jt Surg.* 1962;44(6):1073-1088. doi:10.2106/00004623-

196244060-00004

51. Fahrer M. The thenar eminence: an introduction. In: R. T, ed. *The Hand*. Vol 1. WB Saunders, Philadelphia; 1981:255-258.
52. Woo SL-Y, Gomez MA, Woo Y-K, Akeson WH. Mechanical properties of tendons and ligaments. *Biorheology*. 1982;19(3):397-408.
53. Magnusson SP, Narici M V., Maganaris CN, Kjaer M. Human tendon behaviour and adaptation, in vivo. *J Physiol*. 2008. doi:10.1113/jphysiol.2007.139105
54. Mhanna C, Marquardt TL, Li ZM. Adaptation of the transverse carpal ligament associated with repetitive hand use in pianists. *PLoS One*. 2016. doi:10.1371/journal.pone.0150174
55. Seradge H, Jia YC, Owens W. In vivo measurement of carpal tunnel pressure in the functioning hand. *J Hand Surg Am*. 1995. doi:10.1016/S0363-5023(05)80443-5
56. Li ZM, Fisk JA, Woo SL. The use of the matrix method for the study of human motion: theory and applications. *Sheng wu yi xue gong cheng xue za zhi= J Biomed Eng Shengwu yixue gongchengxue zazhi*. 2003;20(3):375-383.
57. Jacobson MD, Raab R, Fazeli BM, Abrams RA, Botte MJ, Lieber RL. Architectural design of the human intrinsic hand muscles. *J Hand Surg Am*. 1992. doi:10.1016/0363-5023(92)90446-V
58. Schwarzkopf R, DeFrate LE, Li G, Herndon JH. The quantification of the origin area of the deep forearm musculature on the interosseous ligament. *Bull NYU Hosp Jt Dis*. 2008.
59. Pacek CA, Chakan M, Goitz RJ, Kaufmann RA, Li ZM. Morphological analysis of

- the transverse carpal ligament. *Hand*. 2010. doi:10.1007/s11552-009-9219-2
60. Fisk GR. The influence of the transverse carpal ligament (flexor retinaculum) on carpal stability. *Ann Chir la Main*. 1984. doi:10.1016/S0753-9053(84)80003-4
 61. Morrell N, Harris A, Skjong C, Akelman E. Carpal Tunnel Release: Do We Understand the Biomechanical Consequences? *J Wrist Surg*. 2016. doi:10.1055/s-0036-1580088
 62. Brand PW, Beach RB, Thompson DE. Relative tension and potential excursion of muscles in the forearm and hand. *J Hand Surg Am*. 1981. doi:10.1016/S0363-5023(81)80072-X
 63. Viegas SF, Pollard A, Kaminksi K. Carpal arch alteration and related clinical status after endoscopic carpal tunnel release. *J Hand Surg Am*. 1992. doi:10.1016/S0363-5023(09)91048-6
 64. Garcia-Elias M, Sanchez-Freijo JM, Salo JM, Lluch AL. Dynamic changes of the transverse carpal arch during flexion-extension of the wrist: Effects of sectioning the transverse carpal ligament. *J Hand Surg Am*. 1992. doi:10.1016/S0363-5023(09)91049-8
 65. Gartsman GM, Kovach JC, Crouch CC, Noble PC, Bennett JB. Carpal arch alteration after carpal tunnel release. *J Hand Surg Am*. 1986. doi:10.1016/S0363-5023(86)80144-7
 66. Kim DH, Marquardt TL, Gabra JN, et al. Pressure-morphology relationship of a released carpal tunnel. *J Orthop Res*. 2013. doi:10.1002/jor.22271